

# Effect of gas-transfer-velocity parameterization choice on CO<sub>2</sub> air-sea fluxes in the North Atlantic and the European Arctic

Iwona Wrobel<sup>1</sup> and Jacek Piskozub<sup>1</sup>

<sup>1</sup> Institute of Oceanology, Polish Academy of Sciences, Sopot, Poland

*Correspondence to: I. Wróbel (iwrobel@iopan.gda.pl)*

## Abstract

The ocean sink is an important part of the global carbon budget. Understanding uncertainties in the net flux into the ocean is crucial for comprehension the global carbon cycle. One of the sources of the uncertainty is the parameterization for the CO<sub>2</sub> gas transfer velocity. We used a recently developed software tool, FluxEngine, in order to estimate the monthly net carbon air-sea flux for the extratropical North Atlantic, the European Arctic, as well as global values (in order to compare) using several available parameterizations of the gas transfer velocity for different wind speed, both quadratic and cubic. The aim of the study is to constrain the uncertainty caused by the choice of parameterization in the North Atlantic, which is a large sink of CO<sub>2</sub> and the region with a good covering measurement, characterised by strong winds. We show that this uncertainty is smaller in the North Atlantic and the Arctic than globally within 5% in the North Atlantic and 4% in the European Arctic, comparing to 9% for the World Ocean when restricted to functions with quadratic wind dependence and respectively 42%, 40% and 67% for all studied parameterizations. We propose an explanation of this smaller uncertainty caused by combination of higher than global average wind speeds in the North Atlantic and lack of seasonal changes in the flux direction in most of the region. We also compare the available *p*CO<sub>2</sub> datasets (Takahashi and SOCAT), *p*CO<sub>2</sub> discrepancies in the annual fluxes values of 8% in the North Atlantic and 19% in the European Arctic. Seasonality of the flux changes in the Arctic are opposite to one other in both datasets, most likely caused by insufficient data coverage, especially in winter.

## 1. Introduction

The region of extratropical North Atlantic, including the European Arctic, is a region where a large part of ocean deep waters are formed (see Talley (2013) for a recent review). This process, part of the global overturning circulation, makes the area a large sink of CO<sub>2</sub> (Takahashi et al. 2002; Takahashi et al., 2009; Landschützer et al., 2014; Le Quéré et al., 2015), including its anthropogenic fraction (Orr et al., 2001). Therefore, there is a widespread interest in tracking the changes in the North Atlantic carbon fluxes, especially as models predict decreasing the sink volume later this century (Halloran et al., 2015).

The trends in North Atlantic CO<sub>2</sub> sink has been intensively studied since observations have shown it is decreasing (Lefevre et al., 2004). The sink decrease in interannual time scales has been confirmed by further studies (Schuster and Watson, 2007) and continued in recent years North of 40° N (Landschützer et al., 2013). It is not certain how many of these changes are the results of long-term changes, how many of decadal changes in atmospheric forcing, namely the North Atlantic Oscillation (Gonzalez-Davila et al., 2007; Thomas et al., 2008; Gruber 2009; Watson et al., 2009) and changes in meridional overturning circulations (Perez et al., 2013). Recent assessments of the Atlantic and Arctic sea–air CO<sub>2</sub> fluxes (Schuster et al., 2013) and global ocean carbon uptake (Wanninkhof et al., 2013) showed that this problem has not been yet resolved.

Studying the rate of the ocean CO<sub>2</sub> sink and especially its long-terms trends, one needs to constrain the flux uncertainty. Its sources are sampling coverage, the method of data interpolation, in-water fugacity data quality, the method used for normalization of fugacity data to a reference year in a world of ever increasing atmospheric CO<sub>2</sub> partial pressure and the choice of gas transfer velocity  $k$  parameterization (Landschützer et al., 2014; Woolf et al., 2015a, 2015b). In this work we have chosen to analyze various empirical parameterizations using wind speed. Although the North Atlantic is one of the regions of the world ocean best covered by CO<sub>2</sub> fugacity measurements (Watson et al., 2011), the Arctic seas coverage is much poorer, especially in winter (Schuster et al., 2013). It has to be noticed that also the choice of the wind product adds to the uncertainty (Gregg et al., 2015).

One of the factors influencing the value of the calculated air-sea gas flux is the choice of formula for gas transfer velocity. Literature of the subject has several parameterization to choose from different depending on the wind speed (cubic or quadratic). This problem is not trivial as indicated even by the name of one of the meetings on the topic the COST-735 Action organized “ $k$  conundrum” workshop (in Norwich, February 2008). Its results have been incorporated into a recent review book chapter (Garbe et al., 2014). This paper will concentrate on the very uncertainty caused by the choice of the gas flux velocity parameterization in the case of the North Atlantic and the European Arctic. The region was chosen due to being the area of many studies some of the parameterizations were based on and also as a region with wind distribution tilted to higher winds than the global average to test the effect of stronger winds on the difference of net fluxes calculated using the published gas transfer velocity formulas.

## 2. Methods

### 2.1 Datasets

We calculated air-sea carbon dioxide fluxes using a set of processing tools named ‘FluxEngine’ (Shutler et al., 2016) (which is available on the <http://www.ifremer.fr/cersat1/exp/oceanflux/>), created within European Space Agency funded OceanFlux Greenhouse Gases project (Goddijn-Murphy et al., 2015). All calculations were performed using the FluxEngine software, we were only end-users of. The software became publicly available in March 2016 under an open source license, but at the time we started this study we did not have more information about it than is included in the paper describes a set of tools (Shutler et al., 2016). This was a conscious decision because, even as we had access to the toolset developers, we wanted to test it as the end users (this is probably the first study using the toolset by authors who had no part in creating it). The idea, beyond the tool development, was to encourage the use of satellite Earth Observation (EO) data for studying air-sea fluxes. Within the FluxEngine, a suite of reanalyzes, *in situ* and model data are available as input to the toolbox that can be use by the scientific community and to aid the interpretation of the resultant flux data. There is a choice of several different flux parameterization as well as input data, allowing the generation of the monthly global gridded flux products with 1°x1° spatial resolution. The output files contained twelve sets (one set per month) in a NetCDF files. Each data set includes the mean (first order moment), median, standard deviation and the second, third and fourth order moments calculated for each calendar month. There is also information about origin of data inputs as well as results of our calculations. Input data users can choose from all available on the FluxEngine program (perhaps from monthly EO data: rain intensity and event, wind speed and direction, % of sea ice cover from monthly model data ECMWF air pressure, whitecapping (Goddijn-Murphy et al., 2011), from monthly climatology as  $p\text{CO}_2$ , SST, salinity) and configure them in a various way (Shutler et al., 2016). The user needs to choose different components in a calculation process as a

way of computed transfer velocity, parametrization to the wind speed calculation, corrections etc. The FluxEngine has been developed not only to support the study of the air-sea flux of CO<sub>2</sub> but also to aid the study of other gases as DMS and N<sub>2</sub>O (Land et al., 2013; Shutler et al., 2016).

For the calculations, we used  $p\text{CO}_2$  and salinity values from Takahashi et al. (2009) climatology based on more than 3 million measurements of surface water  $p\text{CO}_2$  in open-ocean environments during non El Nino conditions (recalculated to fugacity in the FluxEngine toolset). For some calculations we used, as an alternative, Surface Ocean CO<sub>2</sub> Atlas (SOCAT) ver. 1.5 and 2.0 (Sabine et al., 2013; Pfeil et al., 2013; Bakker et al., 2014)  $p\text{CO}_2$  and SST data. SOCAT is a community driven dataset containing respectively 6.3 and 10.1 million surface water CO<sub>2</sub> fugacity values with a global coverage. The SOCAT databases have been converted to climatologies using methodology described in Goddijn-Murphy, et al. (2015). All the climatologies were calculated for year 2010 within the FluxEngine toolset. The SST values were taken from Operational Sea Surface Temperature and Sea Ice Analysis (OSTIA) (Donlon et al., 2011), and in the case of SOCAT database, while SST skin data that we use come from ARC/(A)ATSR Global Monthly Sea Surface dataset (Merchant et al., 2012). Both data sets have been preprocessed in the same way using the toolsets of FluxEngine (Shutler et al., 2016).

We used Earth Observation (EO) wind speed and sea roughness ( $\sigma_0$  in Ku band from GlobWave L2P products) data obtained from the European Space Agency (ESA) Environmental monitoring satellite, Envisat. Envisat was launched in 2002 with 10 instruments onboard into sun-synchronous near-polar orbit (SSO) with 35 day repeat cycle. It carries, among others, two atmospheric sensors monitoring trace gases. EO data supports earth science research and allows monitoring of the evolution of environmental and climate change.

All the data were used globally within the FluxEngine software. From the gridded product (1 x 1 deg) we extracted the extratropical North Atlantic (North of 30° N), and its subset, the European Arctic (North of 64° N). We use everywhere the convention of sources (upward ocean-to-atmosphere fluxes) being positive and sinks (downward atmosphere-to-ocean fluxes) being negative. We give all results of carbon fluxes in the SI unit of Pg (numerically identical to Gt).

## 2.2. $k$ parameterizations

The flux of CO<sub>2</sub> at the interface of air and the sea is controlled by wind speed, sea state, sea surface temperature (SST) and other factors. We estimate the air-sea flux of CO<sub>2</sub> ( $OF$ , g C m<sup>-2</sup> day<sup>-1</sup>) as the product of gas transfer velocity ( $k$ , ms<sup>-1</sup>) and also the difference in CO<sub>2</sub> concentration (gm<sup>-3</sup>) at the sea water and the interface – air (Land et al., 2013). The concentration of CO<sub>2</sub> in sea water is a product of its solubility ( $\alpha$ , g m<sup>-3</sup>  $\mu\text{atm}^{-1}$ ) and its fugacity ( $f\text{CO}_2$ ,  $\mu\text{atm}$ ). Solubility is in turn, a function of salinity and temperature. Hence Eq. (1) is represented as:

$$F = k (\alpha_W f\text{CO}_{2W} - \alpha_S f\text{CO}_{2A}) \quad (1)$$

where the subscripts denote values in water (W) and the air-sea interface (S) and in the air (A). We can exchange fugacity to the partial pressure (their values differ by <0.5 % over the temperature range considered) (McGillis et al., 2001). So equation (2) now becomes:

$$F = k (\alpha_W p\text{CO}_{2W} - \alpha_S p\text{CO}_{2A}) \quad (2)$$

We can also ignore the differences between the two solubilities and just use the water side solubility  $\alpha_W$ . Equation (3) will be represented as:

$$F = k \alpha_w (p\text{CO}_{2W} - p\text{CO}_{2A}) \quad (3)$$

This formulation is often referred to the ‘bulk parametrization’.

In this work we chose to analyze the fluxes using five different parameterizations, within the FluxEngine software, using in terms of wind speed to parametrized  $k$ . All of them are parameterized with wind speed and differ in the formula for gas transfer velocity,  $k$ :

$$k = \sqrt{(660.0 / \text{Sc}_{\text{skin}}) * (0.212 U_{10}^2 + 0.318 U_{10})} \quad (4)$$

(Nightingale et al., 2000),

$$k = \sqrt{(660.0 / \text{Sc}_{\text{skin}}) * 0.254 U_{10}^2} \quad (5)$$

(Ho et al., 2006),

$$k = \sqrt{(660.0 / \text{Sc}_{\text{skin}}) * 0.0283 U_{10}^3} \quad (6)$$

(Wanninkhof and McGillis, 1999),

$$k = \sqrt{(660.0 / \text{Sc}_{\text{skin}}) * 0.251 U_{10}^2} \quad (7)$$

(Wanninkhof, 2014),

$$k = \sqrt{(660.0 / \text{Sc}_{\text{skin}}) * (3.3 + 0.026 U_{10}^3)} \quad (8)$$

(McGillis et al., 2001),

where the subscripts are Schmidt numbers at the skin surface ( $\text{Sc}_{\text{skin}}$ ), a function of SST ( $[= (\text{kinematic viscosity of water})/(\text{diffusion coefficient of CO}_2 \text{ in water})]$ ), 660.0 is the Schmidt number for carbon dioxide at 20 °C temperature in seawater,  $U_{10}$  is the wind speed 10 m above the sea surface.

In addition to purely wind driven parameterizations, we have used combined Goddijn-Murphy et al. (2012) and Fangohr and Woolf (2007) parametrization, created as part of OceanFlux GHG Evolution project and provided as an option in FluxEngine. This parameterization separates contributions from direct and bubble-mediated gas transfer as suggested by Woolf (2005). Its purpose is to enable a separate evaluation of the effect of the two processes on gas fluxes and should not be treated as the final product (one of the aims of the ongoing OceanFlux Evolution project is improving this parameterization). We used these OceanFluxGHG Evolution parameterizations in two versions: wind driven (using the  $U_{10}$  wind fields) and radar backscatter driven (using mean wave square slope) as described in Goddijn-Murphy et al. (2012).

### 3. Results

Using the FluxEngine software, we have produced CO<sub>2</sub> global monthly gridded air-sea fluxes and calculated from them the values for the study region, the extratropical North Atlantic and separately for its subset, the European Arctic seas. Figure 1 shows maps of the average CO<sub>2</sub> fluxes for the North Atlantic, calculated with Nightingale et al. (2000) (named further as N2000)  $k$  formula and Takahashi et al. (2009) climatology for the whole year and for each season. The area, as a whole, is a carbon sink but even the seasonal maps show that some regions close to North Atlantic Drift and East Greenland Current are net sources. The seasonal maps show even more variability. For example, the above mentioned sinks areas which become sink in summer (effect of phytoplankton blooms) while the southernmost areas of the study become CO<sub>2</sub> sources in summer and autumn (effect of sea-water temperature changes). Much of this variability is caused by changes of the

surface water  $p\text{CO}_2$  average values, shown in Figure 2 for the whole year and for each season (and variability in atmospheric  $\text{CO}_2$  partial pressure, not shown). However, the flux is proportional to the product of  $\Delta p\text{CO}_2$  and  $k$ . In most parameterizations  $k$  is a function of wind speed (eqs. 4-8). The average wind speed  $U_{10}$  for the whole year and each season are shown in Figure 3. The wind speeds in the North Atlantic are higher than the mean in the world ocean, with average values higher than  $10 \text{ m s}^{-1}$  in many regions of the study area in all seasons except for the summer (with highest values in winter). This is important because the fluxes depend not only on average wind speed but also on its distribution (see also the Discussion). This effect is especially visible between formulas with different powers of  $U_{10}$ . Figure 4 shows the difference in the fluxes calculated on the example of two parameterizations: one proportional to  $U_{10}^3$  (eq. 6) and one to  $U_{10}^2$  (eq. 7), namely Wanninkhof and McGillis (1999) and Wanninkhof (2014). It can be seen that the “cubic” function results in higher absolute flux values, compare to a “quadratic” one, in the regions of high winds and lower with weaker winds.

Figure 5 shows the monthly values of  $\text{CO}_2$  fluxes for the five parameterizations (eq. 4-8) for the North Atlantic and the European Arctic. The areas are a sink in every month, although August is close to neutral for the North Atlantic. The results using two cubic formula (eqs. 6 and 8) are higher in absolute values, respectively by up to 30% for Wanninkhof and McGillis (1999) and 55% for McGillis (2001), compare to the “quadratic” N2000 (eq. 4). The other two “quadratic” parameterizations (eqs. 5 and 7) resulted in fluxes within 5% of N2000. Annual fluxes for the North Atlantic and the European Arctic and global (for comparison) are shown in Figure 6. In addition to the five parameterizations, the figure presents results for both the OceanFluxGHG Evolution formulas (using wind and radar backscatter data). The mean and standard deviations of the parametrization ensemble are shown as gray vertical lines. The uncertainty in global fluxes is similar to previous estimates (Sweeney et al., 2007, Landschützer et al., 2014) but they cannot be directly compared due to different parameterization choices and methodologies. The annual North Atlantic fluxes, depending on the formula used, varies from -0.38 PgC for N2000 to -0.56 PgC for McGillis et al. (2001). In the case of global carbon flux the values are, respectively, -1.30 PgC and -2.15 PgC. Figure 7 shows the same data “normalized” to the N2000 (divided by value), the parameterization results in a lower absolute flux values to visualize the relative differences. In the case of the North Atlantic using the “quadratic” Wanninkhof (2014) and Ho et al. (2006) results in a flux respectively 3% and 5% higher in absolute value than N2000, while the “cubic” Wanninkhof and McGillis (1999) and McGillis et al. (2001) results in up to 28% and 42% higher values. The respective values for the Arctic are 3%, 4% for quadratic as well as 27% and 40% for cubic functions. In the case of global flux the respective values are 8% and 9% higher than N2000 flux for the quadratic functions as well as 34% and 67% for cubic ones. The OceanFluxGHG parameterization results in fluxes 18% and 32% higher for North Atlantic than N2000 (for respectively backscatter and wind driven versions). In the case of global values this surplus was, respectively, 45% and 52%.

All the above results used the Takahashi (2009)  $p\text{CO}_2$  climatology. For comparison we have also calculated fluxes using SOCAT version 1.5 and 2.0, interpolated to create a climatology using the FluxEngine toolset (Shutler et al., 2016). Figure 8 shows the results using N2000  $k$  parameterization for all the three climatologies. In the case of the North Atlantic study area, although the monthly values show large differences (using both SOCAT datasets results in a larger sink in summer and smaller in winter compare to Takahashi), the annual values are similar: -0.38 PgC for both Takahashi and SOCAT v.1.5 and -0.41 PgC for SOCAT v. 2.0. In the case of the European Arctic the situation is different, with Takahashi and SOCAT dataset derived climatologies resulting in inverse seasonal variability even as annual flux results are similar: -0.102 PgC for Takahashi, -0.085 PgC for SOCAT v. 1.5 and -0.088 PgC for SOCAT v. 2.0.

#### 4. Discussion

Our results show that using the three “quadratic” parameterizations (Nightingale et al., 2000; Ho et al., 2006 and Wanninkhof 2014) results in fluxes values within 5% of each other in the case of the North Atlantic. This discrepancy is smaller than the 9% difference for the net global carbon air-sea flux (Fig. 7). This would confirm that at present, the parameterizations are interchangeable being all within the experimental uncertainty (Nightingale, 2015). The three parameterizations were derived using different methods and data from different regions, namely passive tracers and dual-trace experiments in the North Sea in the case of Nightingale et al. (2000), dual tracers in the Southern Ocean in the case of Ho et al. (2006) and global ocean  $^{14}\text{C}$  inventories in the case of Wanninkhof (2014). This makes it possible to be highly confident that at least average fluxes calculated with the three formulas are close to the unknown true values. However, the uncertainties are still large and although the quadratic functions are supported by several lines of evidence (see Garbe et. al., 2014 for discussion), other powers are not completely refuted by the available observations. Therefore, it is important to notice that a choice of one of the available cubic functions may lead to net fluxes larger in absolute values up to 33% in the North Atlantic and 50% globally.

The above results imply smaller relative differences between the parameterizations in the North Atlantic than globally. This is interesting because the North Atlantic is the region of strong winds and most of its area there is no seasonal changes in the flux direction (Fig. 1). This is even more surprising if one realizes that at least some of the older parameterizations were developed, based on a smaller wind range than the ones present in the North Atlantic. After analysis of this unexpected fact, using the formula multiplied by the different wind distribution, we have found two reasons for that. First, when comparing quadratic and cubic parameterizations (Fig. 9), it is clear that these cubic ones imply higher fluxes for high winds while quadratic one for weak winds. This difference can be presented in arithmetic terms. Let us assume two functions of wind speed  $U$ ,  $F_1(U)$  quadratic and  $F_2(U)$  cubic:

$$F_1(U) = a U^2, \quad (9)$$

$$F_2(U) = b U^3. \quad (10)$$

The difference between the two functions  $\Delta F$  is equal to:

$$\Delta F = F_2 - F_1 = b U^3 - a U^2 = b U^2 (U - a b^{-1}) = b U^2 (U - U_x) \quad (11)$$

where  $U_x = a b^{-1}$ . The difference is positive for wind speeds greater than  $U_x$  and negative for smaller ones.  $U_x$  is the value of wind speed for which the two functions intersect. In the case of equations (6) and (7),  $a = 0.251$  and  $b = 0.0283$ , implying  $U_x = 8.87 \text{ m s}^{-1}$ . In fact all the functions presented in Fig. 9 have very similar values for wind speeds close to  $9 \text{ m s}^{-1}$ . The value is very close to average wind speeds in the North Atlantic (Fig. 3). This is one of the reasons of small relative net flux differences. The other is lack of seasonality. In case of seasonal changes in the flux direction (caused by seasonal changes in water temperature or primary productivity), with winds stronger than  $U_x$  in some seasons and weaker in other (usually strong winds in winter and weak in summer), the fluxes partly cancel each other while the difference between cubic and quadratic parameterizations add to each other due to simultaneous changes in the sign of both fluxes itself and the  $U - U_x$  term. This effect of seasonality has been suggested to us basing on available data (A. Watson – personal communication) but we are unaware of any paper explaining it in the terms of arithmetic formulas, or even describing it explicitly.

In addition to the five parameterizations described above, we calculated fluxes for the OceanFluxGHG Evolution combined formula, separating contributions from direct and bubble-mediated gas transfer. The resulting fluxes are higher in absolute terms, from all the quadratic functions considered in this study, being closer to cubic ones. This may mean that the bubble mediated term of Fangohr and Woolf (2007) may be an overestimation for CO<sub>2</sub> fluxes. This question will be the subject of further studies in the OceanFlux Evolution project.

Although, using both Takahashi climatology and SOCAT *p*CO<sub>2</sub> dataset (Fig. 8) results in similar annual fluxes in the North Atlantic, it should be noted that they show different seasonal changes. This may have been caused by slightly different time periods of the datasets (SOCAT is more recent). The difference is much larger in the European Arctic due to much worse data spatial coverage and possible interpolation artifacts (Goddijn-Murphy et al., 2015). This discrepancy makes us treat the flux results from the Arctic with much less confidence than the ones for the whole North Atlantic. This situation may improve after SOCAT v.3 which is planned to be released in 2016.

## 5. Conclusions

In this paper we have studied the effect of choice of gas transfer velocity parameterization on the net CO<sub>2</sub> air-sea gas flux volume in the North Atlantic and European Arctic using the recently developed FluxEngine software. The results show that the uncertainty caused by the choice of the *k* formula is smaller in the North Atlantic and in the Arctic than globally. The annual net flux difference caused by the choice of the parameterization is within 5% in the North Atlantic and 4% in the European Arctic, comparing to 9% globally for the studied functions with quadratic wind dependence and respectively up to 42% for North Atlantic, 40% for Arctic and 67% between the cubic and quadratic functions. We explain the smaller North Atlantic variability by the combination of higher than global average wind speeds in the North Atlantic, closer to 9 m s<sup>-1</sup>, the wind speed when most *k* parameterization have similar values and the all-season CO<sub>2</sub> sink conditions in most North Atlantic areas. We compare Takahashi and SOCAT *p*CO<sub>2</sub> datasets finding that although the seasonal variability in the North Atlantic is different, annual net fluxes are within 8% in the North Atlantic and 19% in the European Arctic. The seasonal flux changes in the Arctic have inverse seasonal change in both datasets indicating possible under sampling and therefore the need for more polar *p*CO<sub>2</sub> data before than available at present.

## Acknowledgements

The publication has been financed from the funds of the Leading National Research Centre (KNOW) received by the Centre for Polar Studies for the period 2014-2018; OceanFlux Greenhouse Gases Evolution, a project funded by the European Space Agency, ESRIN Contract No. 4000112091/14/I-LG; and GAME "Growing of Marine Arctic Ecosystem", funded by Narodowe Centrum Nauki grant DEC-2012/04/A/NZ8/00661.

## References

Bakker, D. C. E., Pfeil, B., Smith, K., Hankin, S., Olsen, A., Alin, S. R., Cosca, C., Harasawa, S., Kozyr, A., Nojiri, Y., O'Brien, K. M., Schuster, U., Telszewski, M., Tilbrook, B., Wada, C., Akl, J., Barbero, L., Bates, N. R., Boutin, J., Bozec, Y., Cai, W.-J., Castle, R. D., Chavez, F. P., Chen, L., Chierici, M., Currie, K., de Baar, H. J. W., Evans, W., Feely, R. A., Fransson, A., Gao, Z.,

- Hales, B., Hardman-Mountford, N. J., Hoppema, M., Huang, W.-J., Hunt, C. W., Huss, B., Ichikawa, T., Johannessen, T., Jones, E. M., Jones, S. D., Jutterström, S., Kitidis, V., Körtzinger, A., Landschützer, P., Lauvset, S. K., Lefevre, N., Manke, A. B., Mathis, J. T., Merlivat, L., Metzl, N., Murata, A., Newberger, T., Omar, A. M., Ono, T., Park, G.-H., Paterson, K., Pierrot, D., Ríos, A. F., Sabine, C. L., Saito, S., Salisbury, J., Sarma, V. V. S. S., Schlitzer, R., Sieger, R., Skjelvan, I., Steinhoff, T., Sullivan, K. F., Sun, H., Sutton, A. J., Suzuki, T., Sweeney, C., Takahashi, T., Tjiputra, J., Tsurushima, N., van Heuven, S. M. A. C., Vandemark, D., Vlahos, P., Wallace, D. W. R., Wanninkhof, R., and Watson, A. J.: An update to the Surface Ocean CO<sub>2</sub> Atlas (SOCAT version 2), *Earth Syst. Sci. Data*, 6, 69-90, doi:10.5194/essd-6-69-2014, 2014.
- Donlon, C. J., Martin, M., Stark, J. D., Roberts-Jones, J., Fiedler, E., and Wimmer, W.: The Operational Sea Surface Temperature and Sea Ice Analysis (OSTIA), *Remote Sens. Environ.*, Special Issue 116, 140-158, doi: 10.1016/j.rse.2010.10.017, 2011.
- Fangohr, S. and Woolf, D. K.: Application of new parameterizations of gas transfer velocity and their impact on regional and global CO<sub>2</sub> budgets, *J. Marine Syst.*, 66, 195-203, 2007.
- Garbe, C. S., Rutgersson, A., Boutin, J., de Leeuw, G., Delille, B., Fairall, C. W., Gruber, N., Hare, J., Ho, D. T., Johnson, M. T., Nightingale, P. D., Pettersson, H., Piskozub, J., Sahlee, E., Tsai, W., Ward, B., Woolf, D. K., and Zappa, C. J.: Transfer Across the Air-Sea Interface, in: *Ocean-Atmosphere Interactions of Gases and Particles*, edited by: Liss, P. S. and Johnson, M. T., Springer, Earth System Science, Springer, Berlin, Heidelberg, 55–111, 2014.
- Goddijn-Murphy L., Woolf D. K., Callaghan A. H.: Parameterizations and Algorithms for Oceanic Whitecap Coverage, *J. Phys. Oceanogr.*, 41, 742-756, 2011.
- Goddijn-Murphy, L. M., Woolf, D. K., and Marandino, C.: Space-based retrievals of air-sea gas transfer velocities using altimeters: Calibration for dimethyl sulfide, *J. Geophys. Res.*, 117, C08028, doi: 10.1029/2011JC007535, 2012.
- Goddijn-Murphy, L. M., Woolf, D. K., Land, P. E., Shutler J. D., Donlon, C.: The OceanGlux Greenhouse Gases methodology for deriving a sea surface climatology of CO<sub>2</sub> fugacity in support of air-sea gas lux studies, *Ocean Sci.*, 11, 519-541, 2015, doi: 10.5194/os-11-519-2015, 2015.
- Gonzalez-Davila, M., Santana-Casiano, J. M., and Gonzalez-Davila, E. F.: Interannual variability of the upper ocean carbon cycle in the northeast Atlantic Ocean, *Geophys. Res. Lett.*, 34, L07608, doi: 10.1029/2006GL028145, 2007.
- Gregg, W. W., Casey N. W., Rosseaux C. S.: Sensitivity of simulated global ocean carbon flux estimates to forcing by reanalysis products, *Ocean Modelling*, 80, 24-35, doi: 10.1016/j.ocemod.2014.05.002, 2015.
- Gruber, N.: Fickle trends in the ocean, *Nature*, 458, 155-156, doi: 10.1038/458155a, 2009.
- Halloran, P. R., Booth, B. B. B., Jones, C. D., Lambert, F. H., McNeall, D. J., Totterdell, I. J., and Völke, C.: The mechanisms of North Atlantic CO<sub>2</sub> uptake in a large Earth System Model ensemble, *Biogeosciences*, 12, 4497–4508, doi: 10.5194/bg-12-4497-2015, 2015.
- Ho, D., Law C., Smith M., Schlosser P., Harvey M., Hill P.: Measurements of air-sea gas exchange at high wind speeds in the Southern Ocean: Implications for global parametrizations, *Geophys.*



Res. Lett., 33, L16611, doi: 10.1029/2006/GL026817, 2006.

Landschützer, P., Gruber, N., Bakker, D. C. E., Schuster, U., Nakaoka, S., Payne, M. R., Sasse, T. P., and Zeng, J.: A neural network-based estimate of the seasonal to inter-annual variability of the Atlantic Ocean carbon sink, *Biogeosciences*, 10, 7793-7815, doi: 10.5194/bg-10-7793-2013, 2013.

Landschützer, P., Gruber, N., Bakker, D. C. E., Schuster, U.: Recent variability of the global ocean carbon sink, *Global Biogeochem. Cy*, 28, 927–949, doi: 10.1002/2014GB004853, 2014.

Le Quéré, C., Moriarty, R., Andrew, R. M., Peters, G. P., Ciais, P., Friedlingstein, P., Jones, S. D., Sitch, S., Tans, P., Arneeth, A., Boden, T. A., Bopp, L., Bozec, Y., Canadell, J. G., Chini, L. P., Chevallier, F., Cosca, C. E., Harris, I., Hoppema, M., Houghton, R. A., House, J. I., Jain, A. K., Johannessen, T., Kato, E., Keeling, R. F., Kitidis, V., Klein Goldewijk, K., Koven, C., Landa, C. S., Landschützer, P., Lenton, A., Lima, I. D., Marland, G., Mathis, J. T., Metzl, N., Nojiri, Y., Olsen, A., Ono, T., Peng, S., Peters, W., Pfeil, B., Poulter, B., Raupach, M. R., Regnier, P., Rödenbeck, C., Saito, S., Salisbury, J. E., Schuster, U., Schwinger, J., Séférian, R., Segsneider, J., Steinhoff, T., Stocker, B. D., Sutton, A. J., Takahashi, T., Tilbrook, B., van der Werf, G. R., Viovy, N., Wang, Y.-P., Wanninkhof, R., Wiltshire, A., and Zeng, N.: Global carbon budget 2014, *Earth Syst. Sci. Data*, 7, 47–85, doi: 10.5194/essd-7-47-2015, 2015.

Lefevre, N., Watson, A. J., Olsen, A., Rios, A. F., Perez, F. F., Johannessen, T.: A decrease in the sink for atmospheric CO<sub>2</sub> in the North Atlantic, *Geophys. Res. Lett.*, 31, L07306, doi: 10.1029/2003GL018957, 2004.

McGillis, W. R., and Edson, J. B., Hare, J. E., Fairall, C. W.: Direct covariance air-sea CO<sub>2</sub> fluxes, *J. Geophys. Res.*, 106, 729-16, 2001.

Merchant, C. J., Embury, O., Rayner, N. A., Berry, D. I., Corlett, G. K., K., L., Veal, K. L., Kent, E. C., T., L.-J. D., Remedios, J. J., and Saunders, R.: A 20 year independent record of sea surface temperature for climate from Along-Track Scanning Radiometers, *J. Geophys. Res.*, 117, 2012.

Nightingale, P. D., Malin, G., Law, C. S., Watson, A. J., Liss, P. S., Liddicoat, M. I., Boutin, J., and Upstill-Goddard, R. C.: In situ evaluation of air-sea gas exchange parametrizations using novel conservative and volatile tracers, *Global Biogeochem. Cy.*, 14, 373-387, 2000.

Nightingale, P. D., Relationship between wind speed and gas exchange over the ocean: which parameterisation should I use?, Raport from Discussion Session at SOLAS Open Science conference in Kiel, <http://goo.gl/TrMQkg>, 2015.

Orr, J. C., Maier-Reimer, E., Mikolajewicz, U., Monfray, P., Sarmiento, J. L., Toggweiler, J. R., Taylor, N. K., Palmer, J., Gruber, N., Sabine, C. L., Quéré, C. Le., Key, R. M., Boutin, J.: Estimates of anthropogenic carbon uptake from four three-dimensional global ocean models, *Global Biogeochem. Cy.*, 15(1), 43-60, doi: 10.1029/2000GB001273, 2001.

Pérez, F. F., Herlé Mercier, Marcos Vázquez-Rodríguez, Pascale Lherminier, Anton Velo, Paula C. Pardo, Gabriel Rosón and Aida F. Ríos: Atlantic Ocean CO<sub>2</sub> uptake reduced by weakening of the meridional overturning circulation, *Nat. Geosci.*, 6, 146-152, doi: 10.1038/NGEO1680, 2013.

Pfeil, B., Olsen, A., Bakker, D. C. E., Hankin, S., Koyuk, H., Kozyr, A., Malczyk, J., Manke, A.,

Metzl, N., Sabine, C. L., Akl, J., Alin, S. R., Bates, N., Bellerby, R. G. J., Borges, A., Boutin, J., Brown, P. J., Cai, W.-J., Chavez, F. P., Chen, A., Cosca, C., Fassbender, A. J., Feely, R. A., González-Dávila, M., Goyet, C., Hales, B., Hardman-Mountford, N., Heinze, C., Hood, M., Hoppema, M., Hunt, C. W., Hydes, D., Ishii, M., Johannessen, T., Jones, S. D., Key, R. M., Körtzinger, A., Landschützer, P., Lauvset, S. K., Lefevre, N., Lenton, A., Lourantou, A., Merlivat, L., Midorikawa, T., Mintrop, L., Miyazaki, C., Murata, A., Nakadate, A., Nakano, Y., Nakaoka, S., Nojiri, Y., Omar, A. M., Padin, X. A., Park, G.-H., Paterson, K., Perez, F. F., Pierrot, D., Poisson, A., Ríos, A. F., Santana-Casiano, J. M., Salisbury, J., Sarma, V. V. S. S., Schlitzer, R., Schneider, B., Schuster, U., Sieger, R., Skjelvan, I., Steinhoff, T., Suzuki, T., Takahashi, T., Tedesco, K., Telszewski, M., Thomas, H., Tilbrook, B., Tjiputra, J., Vandemark, D., Veness, T., Wanninkhof, R., Watson, A. J., Weiss, R., Wong, C. S., and Yoshikawa-Inoue, H.: A uniform, quality controlled Surface Ocean CO<sub>2</sub> Atlas (SOCAT), *Earth Syst. Sci. Data*, 5, 125-143, doi: 10.5194/essd-5-125-2013, 2013.

Sabine, C. L., Hankin, S., Koyuk, H., Bakker, D. C. E., Pfeil, B., Olsen, A., Metzl, N., Kozyr, A., Fassbender, A., Manke, A., Malczyk, J., Akl, J., Alin, S. R., Bellerby, R. G. J., Borges, A., Boutin, J., Brown, P. J., Cai, W.-J., Chavez, F. P., Chen, A., Cosca, C., Feely, R. A., González-Dávila, M., Goyet, C., Hardman-Mountford, N., Heinze, C., Hoppema, M., Hunt, C. W., Hydes, D., Ishii, M., Johannessen, T., Key, R. M., Körtzinger, A., Landschützer, P., Lauvset, S. K., Lefevre, N., Lenton, A., Lourantou, A., Merlivat, L., Midorikawa, T., Mintrop, L., Miyazaki, C., Murata, A., Nakadate, A., Nakano, Y., Nakaoka, S., Nojiri, Y., Omar, A. M., Padin, X. A., Park, G.-H., Paterson, K., Perez, F. F., Pierrot, D., Poisson, A., Ríos, A. F., Salisbury, J., Santana-Casiano, J. M., Sarma, V. V. S. S., Schlitzer, R., Schneider, B., Schuster, U., Sieger, R., Skjelvan, I., Steinhoff, T., Suzuki, T., Takahashi, T., Tedesco, K., Telszewski, M., Thomas, H., Tilbrook, B., Vandemark, D., Veness, T., Watson, A. J., Weiss, R., Wong, C. S., and Yoshikawa-Inoue, H.: Surface Ocean CO<sub>2</sub> Atlas (SOCAT) gridded data products, *Earth Syst. Sci. Data*, 5, 145-153, doi: 10.5194/essd-5-145-2013, 2013.

Schuster, U., and Watson, A. J.: A variable and decreasing sink for atmospheric CO<sub>2</sub> in the North Atlantic, *J. Geophys. Res.*, 112, C11006, doi: 10.1029/2006JC003941, 2007.

Schuster, U., McKinley, G. A., Bates, N., Chevallier, F., Doney, S. C., Fay, A. R., Gonzalez-Davila, M., Gruber, N., Jones, S., Krijnen, J., Landschutzer, P., Lefevre, N., Manizza, M., Mathis, J., Metzl, N., Olsen, A., Rios, A. F., Rodenbeck, C., Santana-Casiano, J. M., Takahashi, T., Wanninkhof, R., and Watson, A. J.: An assessment of the Atlantic and Arctic sea-air CO<sub>2</sub> fluxes, 1990–2009, *Biogeosciences*, 10, 607–627, doi: 10.5194/bg-10-607-2013, 2013.

Shutler, J. D., Piolle, J-F., Land, P. E., Woolf, D. K., Goddijn-Murphy, L., Paul, F., Girard-Ardhuin, F., Chapron, B., and Donlon, C. J.: FluxEngine: a flexible processing system for calculating air-sea carbon dioxide gas fluxes and climatologies, *J. Atmos. Ocean. Tech.*, <http://dx.doi.org/10.1175/JTECH-D-14-00204.1>, 2016.

Sweeney, C., Gloor, E., Jacobson, A. R., Key, R. M., McKinley, G., Sarmiento, J. L. and Wanninkhof, R.: Constraining global air-sea gas exchange for CO<sub>2</sub> with recent bomb 14C measurements, *Global Biogeochem. Cycles*, 21, GB2015, <http://dx.doi.org/10.1029/2006GB002784>, 2007.

Takahashi, T., Sutherland, S. G., Sweeney, C., Poisson, A. P., Metzl, N., Tilbrook, B., Bates, N. R., Wanninkhof, R., Feely, R. A., Sabine, C. L., Olafsson, J., and Nojiri, Y.: Global sea-air CO<sub>2</sub> flux based on climatological surface ocean pCO<sub>2</sub>, and seasonal biological and temperature effects, *Deep Sea Res.*, Pt. II, 49, 1601-1622, 2002.

511  
512 Takahashi, T., Sutherland, S. C., Wanninkhof, R., Sweeney, C., Feely, R. A., Chipman, D. W., Hales,  
513 B., Friederich, G., Chavez, F., Sabine, C., Watson, A., Bakker, D. C. E., Schuster, U., Metzl, N.,  
514 Inoue, H. Y., Ishii, M., Midorikawa, T., Nojiri, Y., Koertzing, A., Steinhoff, T., Hoppema, M.,  
515 Olafsson, J., Arnarson, T. S., Tilbrook, B., Johannessen, T., Olsen, A., Bellerby, R., Wong, C. S.,  
516 Delille, B., Bates, N. R., and de Baar, H. J. W.: Climatological mean and decadal change in  
517 surface ocean  $p\text{CO}_2$  and net sea-air  $\text{CO}_2$  flux over the global oceans, *Deep-Sea Res. Pt. II*, 56,  
518 554–577, doi: 10.1016/j.dsr2.2008.12.009, 2009.  
519  
520 Talley, L. D.: Closure of the Global Overturning Circulation Through the Indian, Pacific, and  
521 Southern Oceans: Schematics and Transports, *Oceanography* 26(1), 80–97,  
522 doi:10.5670/oceanog.2013.07, 2013.  
523  
524 Thomas, H., Friederike Prowe, A. E., Lima, I. D., Doney, S. C., Wanninkhof, R., Greatbatch, R. J.,  
525 Schuster, U., and Corbiere, A.: Changes in the North Atlantic Oscillation influence  $\text{CO}_2$  uptake  
526 in the North Atlantic over the past 2 decades, *Global Biogeochem. Cy.*, 22, GB4027,  
527 doi:10.1029/2007GB003167, 2008.  
528  
529 Wanninkhof, R.: Relationship between wind speed and gas exchange over the ocean revisited,  
530 *Limnol. Oceanogr.- Meth.*, 12, 351–362, 2014.  
531  
532 Wanninkhof, R., and McGillis, W. R.: A cubic relationship between air-sea  $\text{CO}_2$  exchange and wind  
533 speed, *Geophys. Res. Lett.*, 26, 1889–1892, 1999.  
534  
535 Wanninkhof, R., Park, G.-H., Takahashi, T., Sweeney, C., Feely, R., Nojiri, Y., Gruber, N., Doney,  
536 S. C., McKinley, G. A., Lenton, A., Quéré C. Le, Heinze, C., Schwinger, J., Graven, H.,  
537 Khatiwala, S.: Global ocean carbon uptake: magnitude, variability and trends, *Biogeosciences*,  
538 10, 1987–2013, doi: 10.5194/bg-10-1987-2013, 2013.  
539  
540 Watson, A. J., Schuster, U., Bakker, D. C. E., Bates, N. R., Corbière, A., González-Dávila, M.,  
541 Friedrich, T., Hauck, J., Heinze, C., Johannessen, T., Körtzinger, A., Metzl, N., Olafsson, J.,  
542 Olsen, A., Oschlies, A., Padin, X.A., Pfeil, B., Santana-Casiano, J.M., Steinhoff, T., Telszewski,  
543 M., Rios, A.F., Wallace, D.W., Wanninkhof, R.: Tracking the variable North Atlantic sink for  
544 atmospheric  $\text{CO}_2$ , *Science*, 326(5958), 1391–1393, doi: 10.1126/science.1177394, 2009.  
545  
546 Watson, A. J., Metzl, N., Schuster, U.: Monitoring and interpreting the ocean uptake of atmospheric  
547  $\text{CO}_2$ , *Philos. T. R. Soc. A*, 369, 1997–2008, doi: 10.1098/rsta.2011.0060, 2011.  
548  
549 Woolf, D. K.: Parameterization of gas transfer velocities and sea-state dependent wave breaking.  
550 *Tellus B*, 57, 87–94, 2005.  
551  
552 Woolf, D. K., Shutler, J. D., Goddijn-Murphy, L., Donlon, C. J., Nightingale, P. D., Land, P. E.,  
553 Torres, R., Chapron, B., Piolle, J.-F., Herledan, S., Hanafin, J., Girard-Ardhuin, F., Ardhuin, F.,  
554 Prytherch, J., Moat, B., and Yelland, M.: Key uncertainties in the contemporary air-sea flux of  
555 carbon dioxide: an OceanFlux study, submitted 2015a.  
556  
557 Woolf, D. K., Goddijn-Murphy, L. M., Shutler, J. D., Land, P. E., Donlon, C. J., Prytherch, J.,  
558 Yelland, M. J., Nightingale, P. D., Torres, R., Chapron, B., Piolle, J.-F., Herledan, S., Hanafin, J.,  
559 Girard-Ardhuin, F., Ardhuin F., and Moat, B.: Sources and types of uncertainty in the  
560 contemporary air-sea flux of carbon dioxide: an OceanFlux study, submitted 2015b.

561 Figure 1. Seasonal and annual mean air-sea fluxes of  $\text{CO}_2$  ( $\text{mg C m}^{-2} \text{ day}^{-1}$ ) in the North Atlantic,  
562 combine using Nightingale et al. (2000)  $k$  parameterization and Takahashi (2009) climatology in a)   
563 annual, b) DJF (Winter), c) MAM (Spring), d) JJA (Summer), e) SON (Autumn). The gaps (white  
564 areas) are due to missing data, land and ice masks and interpolation algorithms of the FluxEngine  
565 software.  
566

567 Figure 2. Seasonal and annual  $p\text{CO}_2$  values ( $\mu\text{atm}$ ) in surface waters of the North Atlantic,  
568 estimated using Takahashi (2009) climatology in a) annual, b) DJF (Winter), c) MAM (Spring), d)  
569 JJA (Summer), e) SON (Autumn). The gaps (white areas) are due to missing data, land and ice  
570 masks and interpolation algorithms of the FluxEngine software.  
571

572 Figure 3. Wind speed distribution  $U_{10}$  ( $\text{ms}^{-2}$ ) in the North Atlantic used to determine the  
573 relationship between gas transfer velocity and air-sea  $\text{CO}_2$  fluxes in a) annual, b) DJF (Winter), c)  
574 MAM (Spring), d) JJA (Summer), e) SON (Autumn). The gaps (white areas) are due to missing  
575 data, land and ice masks and interpolation algorithms of the FluxEngine software.  
576

577 Figure 4. Differences maps for the air-sea  $\text{CO}_2$  fluxes ( $\text{mg C m}^{-2} \text{ day}^{-1}$ ) in the North Atlantic,  
578 between a wind cubed and squared parameterizations (Wanninkhof and McGillis 1999 and  
579 Wanninkhof 2014) in a) annual, b) DJF (Winter), c) MAM (Spring), d) JJA (Summer) e) SON  
580 (Autumn). The gaps (white areas) are due to missing data, land and ice masks and interpolation  
581 algorithms of the FluxEngine software.  
582

583 Figure 5. Monthly values air-sea fluxes of  $\text{CO}_2$  ( $\text{Pg/month}$ ) for the five parameterizations (eq. 4-8)  
584 in a) North Atlantic, b) European Arctic.  
585

586 Figure 6. Annual air-sea fluxes of  $\text{CO}_2$  ( $\text{Pg/year}$ ) for the five (eq. 4-8) parameterizations as well as  
587 for backscatter (default) and wind driven OceanFluxGHG parameterization (see text) in a) global, b)  
588 North Atlantic c) European Arctic. Average values for all parameterization and standard deviations  
589 are marked as vertical gray lines.  
590

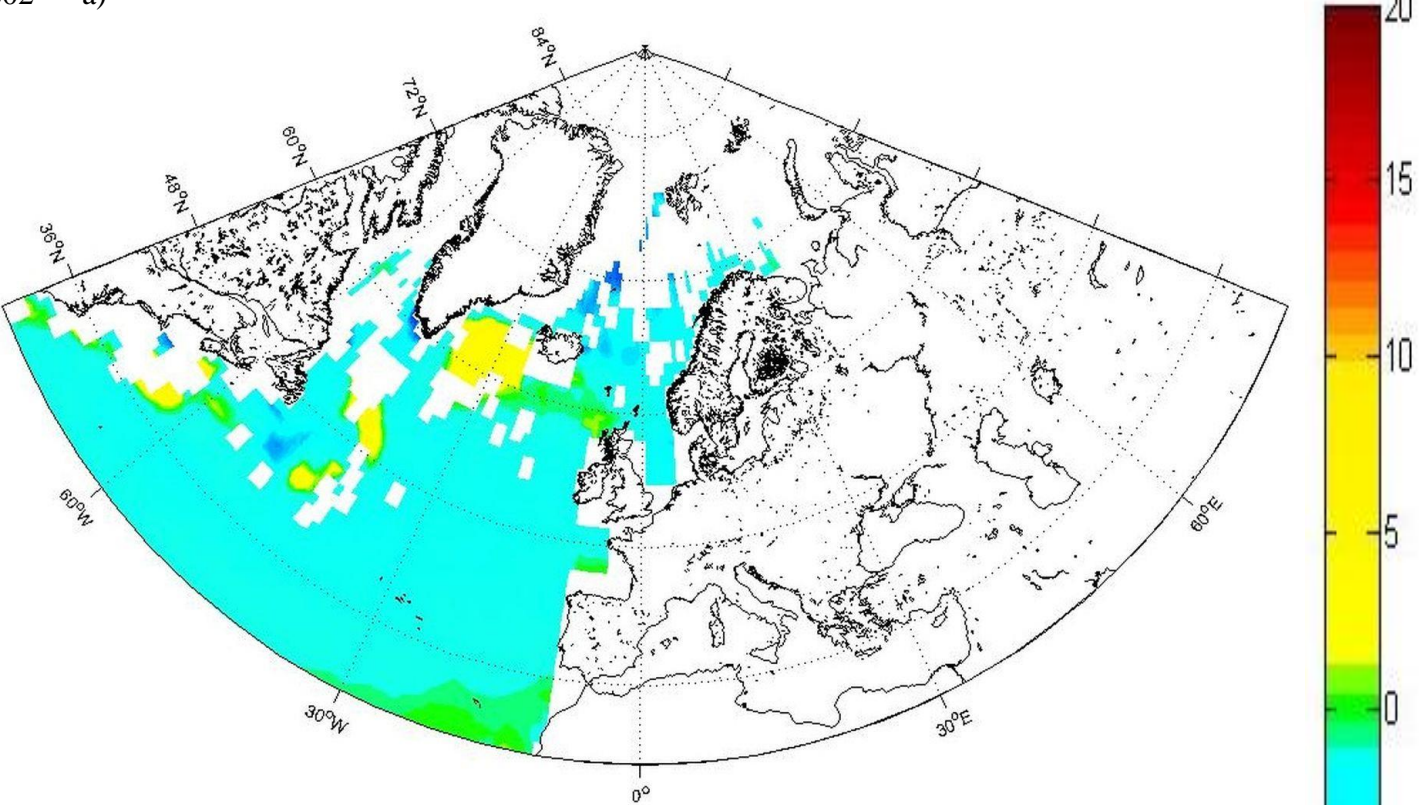
591 Figure 7. Annual air-sea fluxes of  $\text{CO}_2$  for the five (eq. 4-8) parameterizations as well as for  
592 backscatter (default) and wind driven OceanFluxGHG parameterization normalized to flux values  
593 of Nightingale et al. (2000)  $k$  parameterization.  
594

595 Figure 8. Comparison of monthly values fluxes of air-sea  $\text{CO}_2$  fluxes calculated with different  $p\text{CO}_2$   
596 datasets (Takahashi et al. 2009, SOCAT v. 1.5 and 2.0) using the same  $k$  parameterization  
597 (Nightingale et al. 2000) in a) North Atlantic, b) European Arctic.  
598

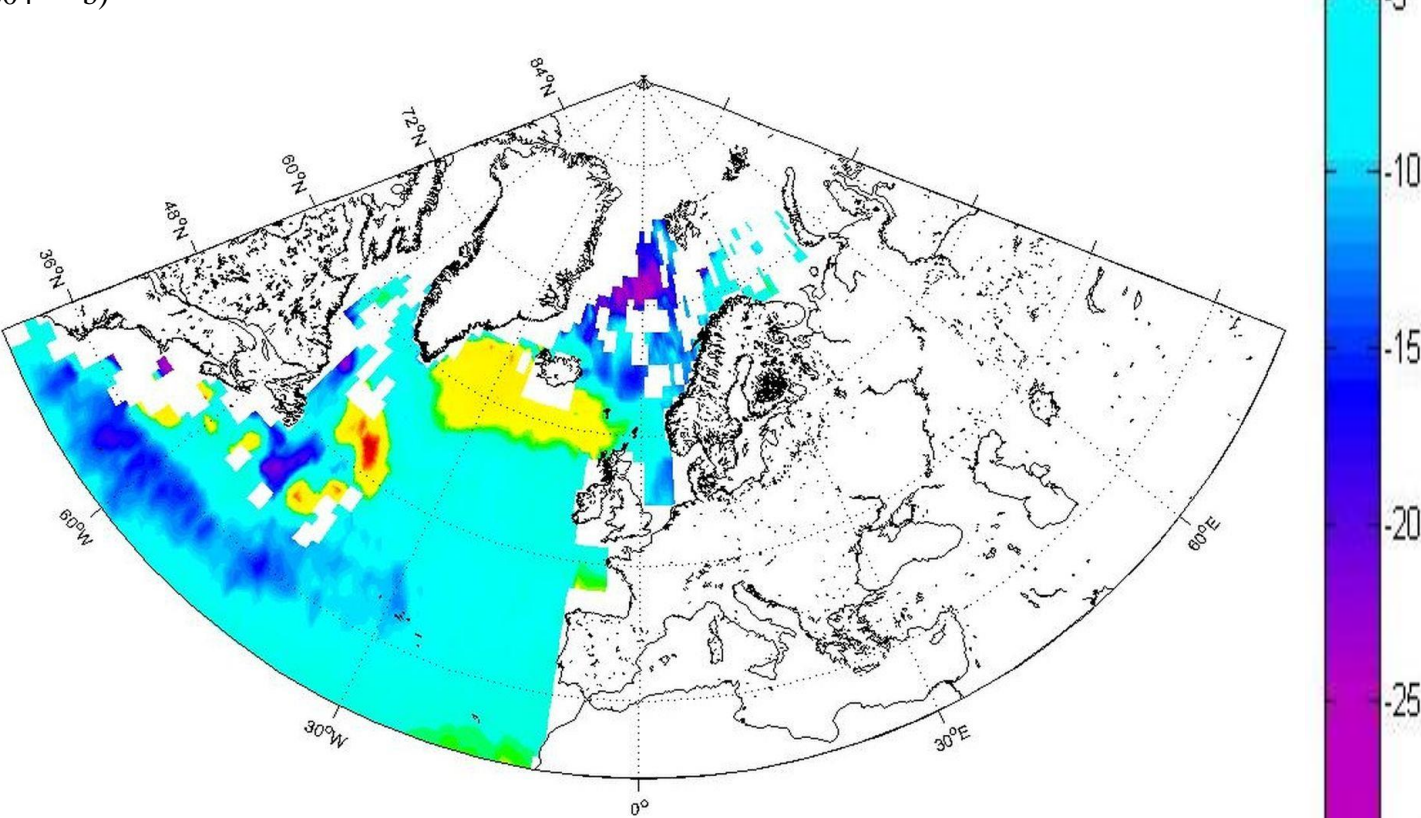
599 Figure 9. Different  $k_{660}$  parameterizations as a function of wind speed.  
600



601  
602 a)



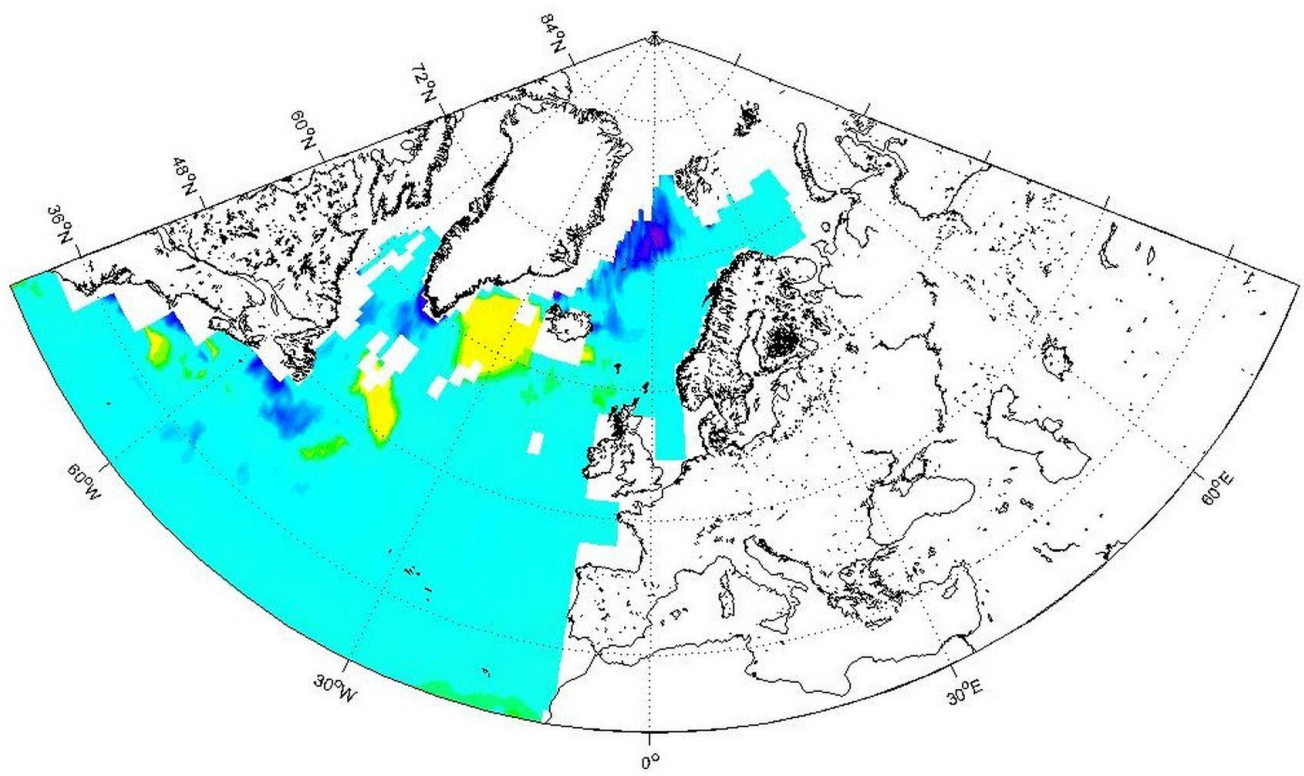
603  
604 b)



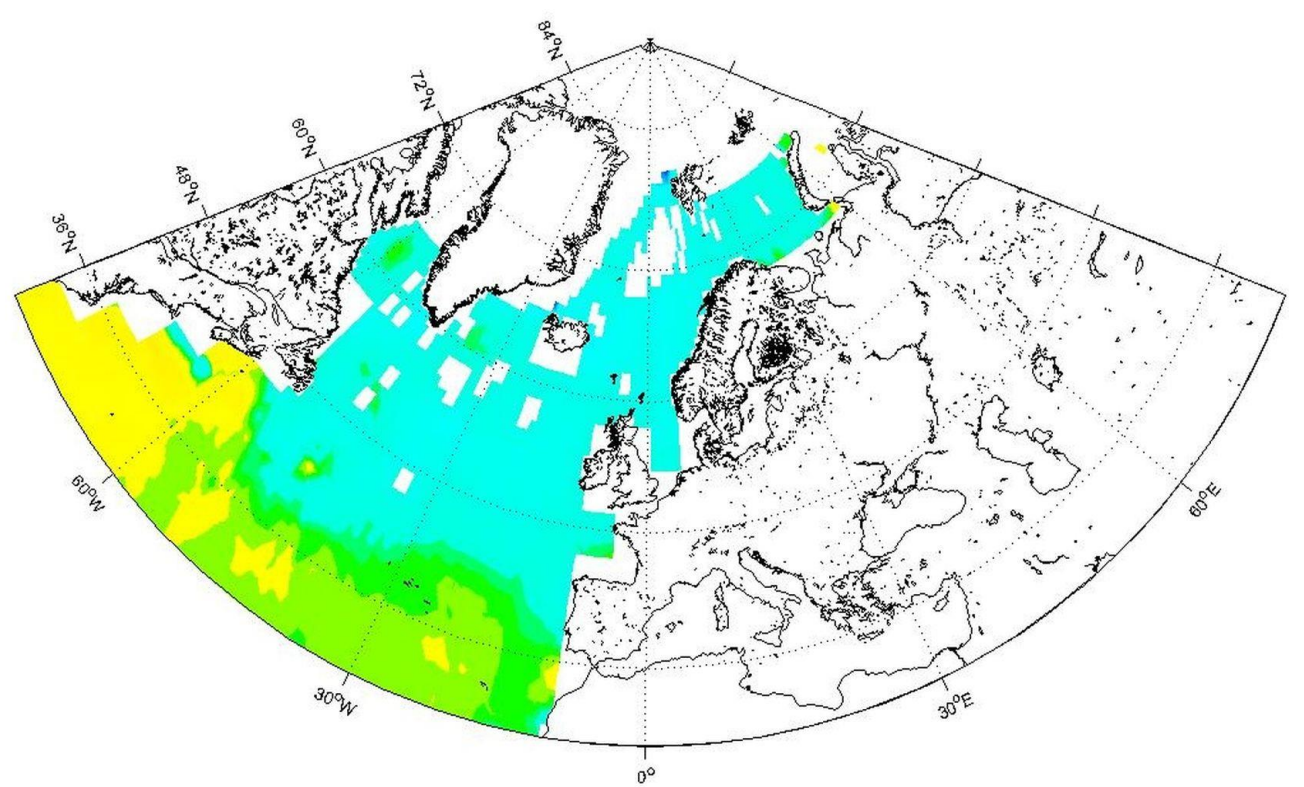
605  
606

(mg C m<sup>-2</sup> day<sup>-1</sup>)

607  
608 c)



609  
610 d)

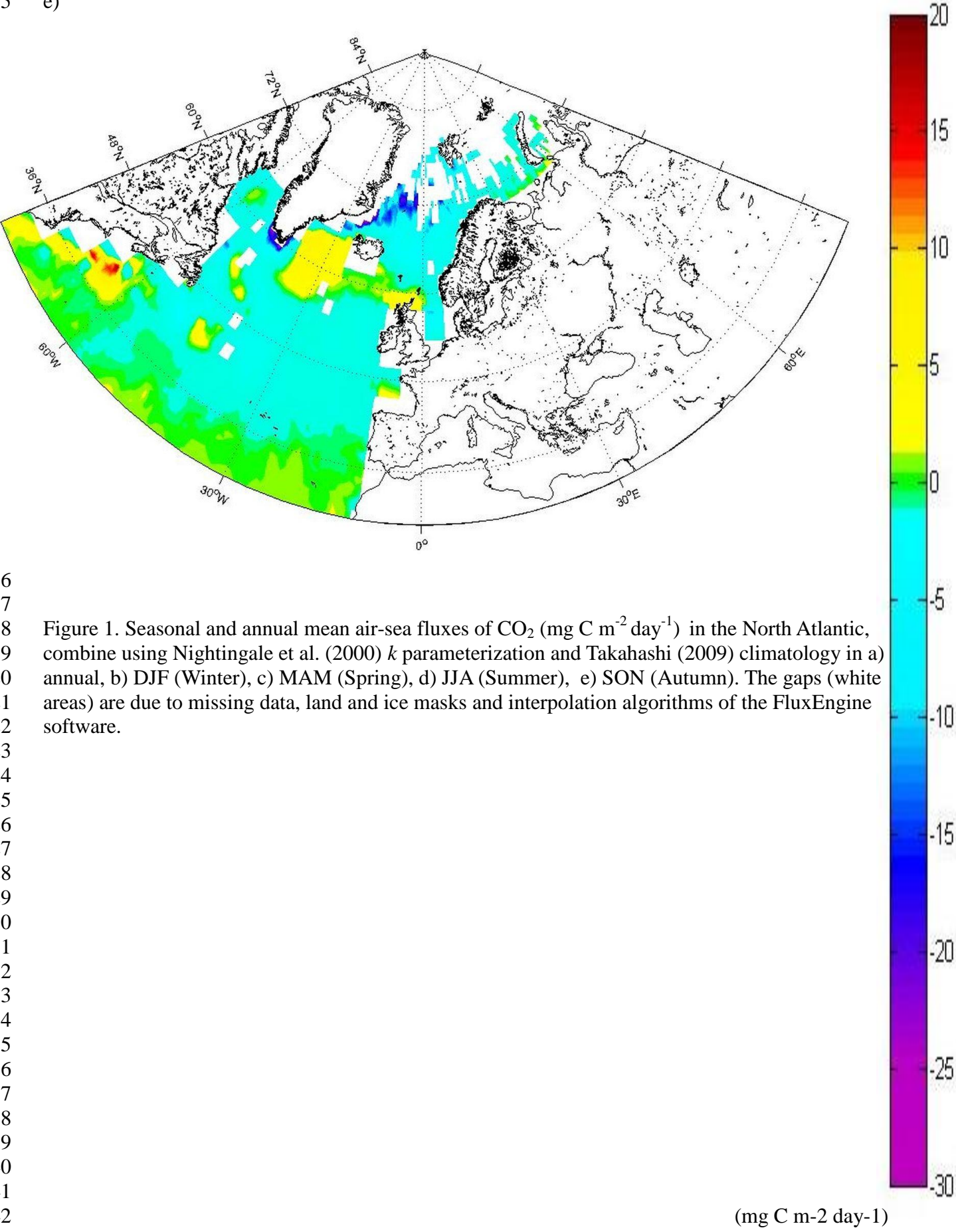


611  
612  
613

(mg C m-2 day-1)



614  
615 e)

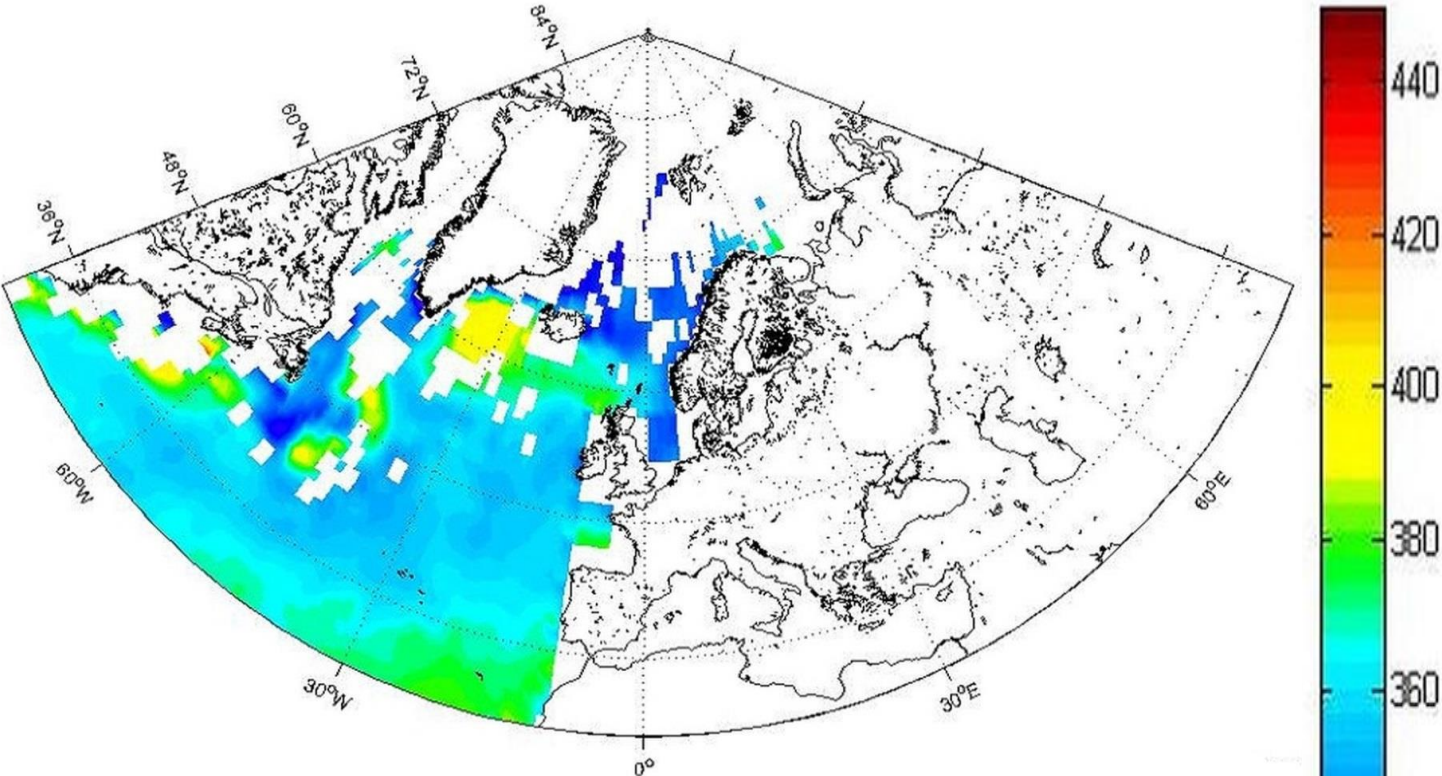


616  
617  
618 Figure 1. Seasonal and annual mean air-sea fluxes of CO<sub>2</sub> (mg C m<sup>-2</sup> day<sup>-1</sup>) in the North Atlantic,  
619 combine using Nightingale et al. (2000) *k* parameterization and Takahashi (2009) climatology in a)  
620 annual, b) DJF (Winter), c) MAM (Spring), d) JJA (Summer), e) SON (Autumn). The gaps (white  
621 areas) are due to missing data, land and ice masks and interpolation algorithms of the FluxEngine  
622 software.

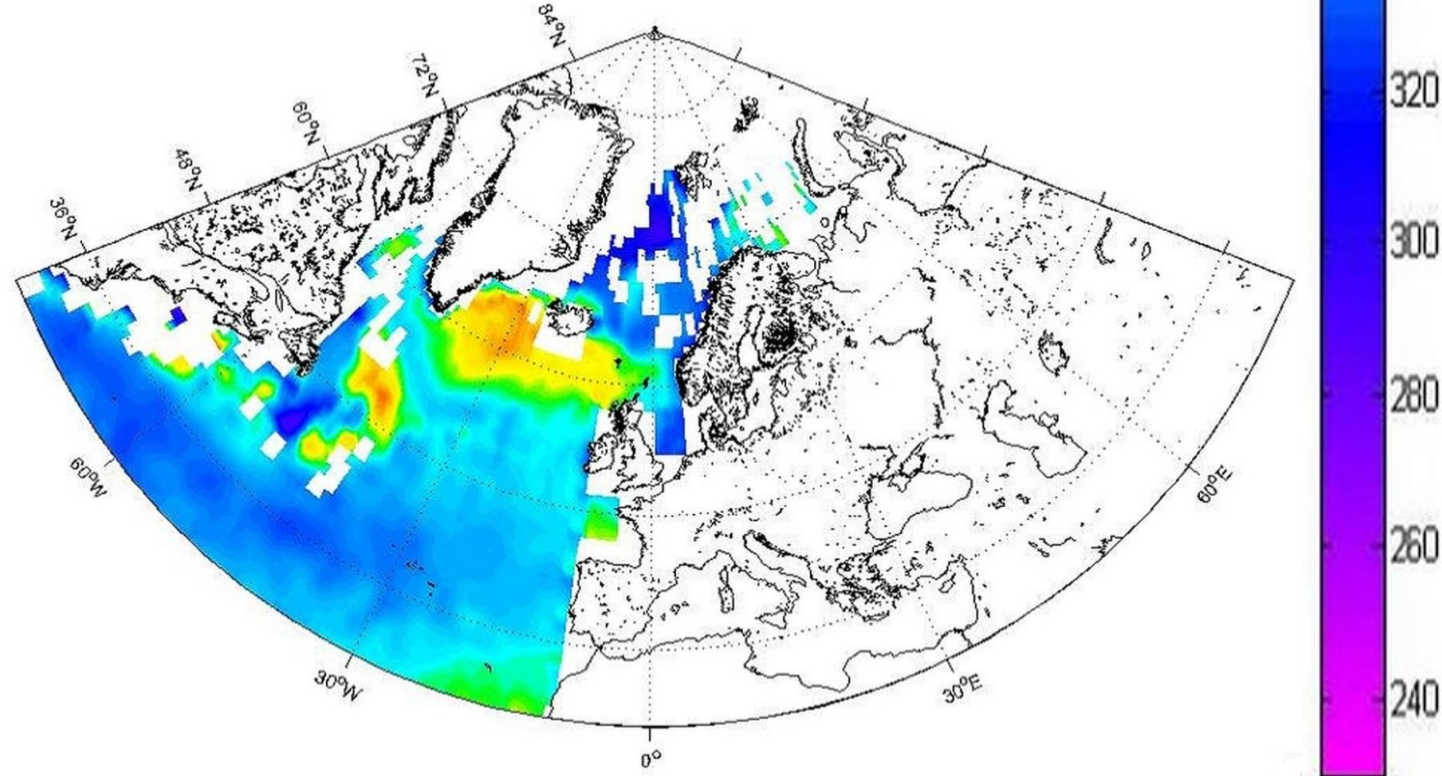
623  
624  
625  
626  
627  
628  
629  
630  
631  
632  
633  
634  
635  
636  
637  
638  
639  
640  
641  
642

(mg C m<sup>-2</sup> day<sup>-1</sup>)

643  
644 a)



645  
646 b)

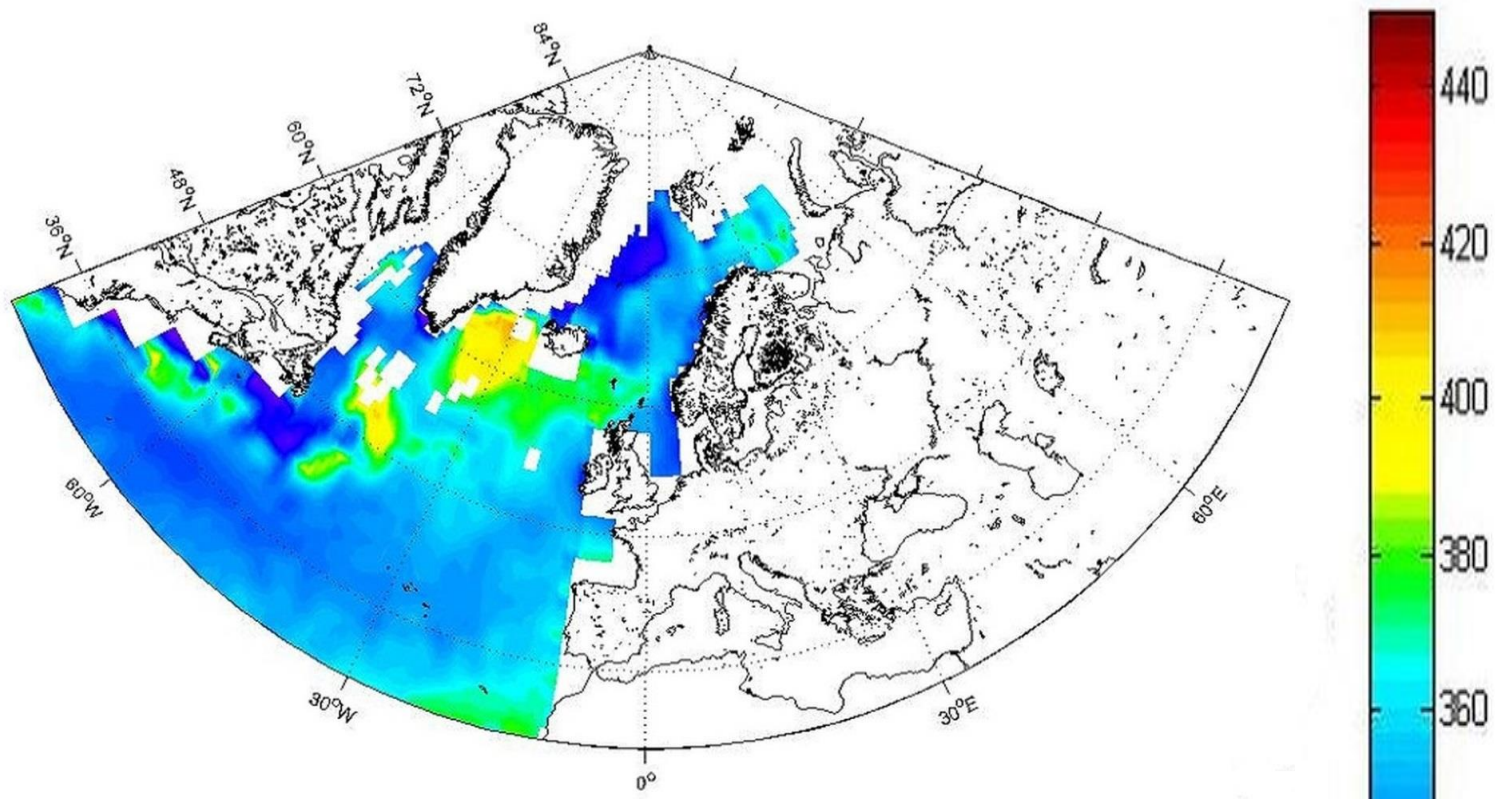


647  
648

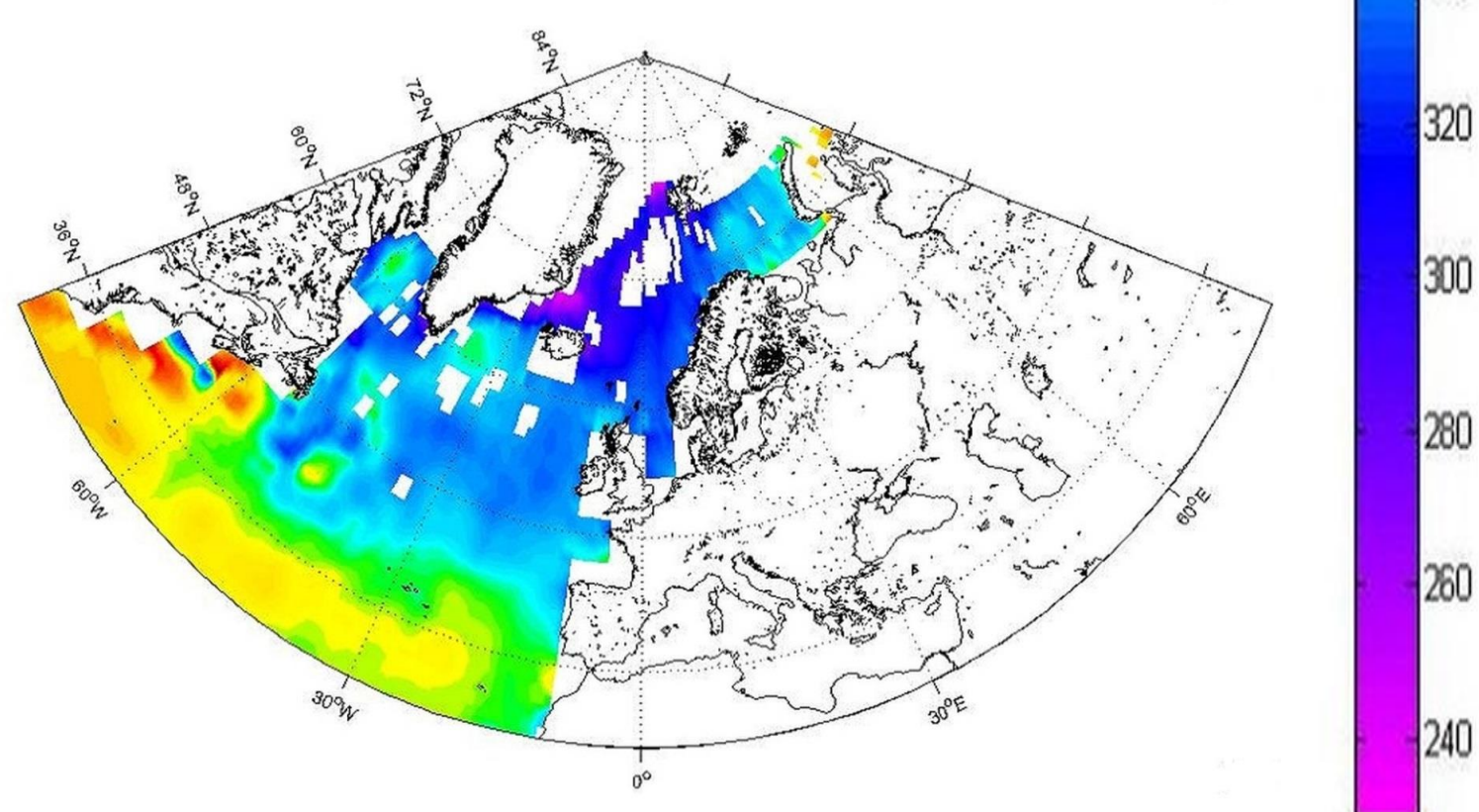
(microatm)



649  
650 c)



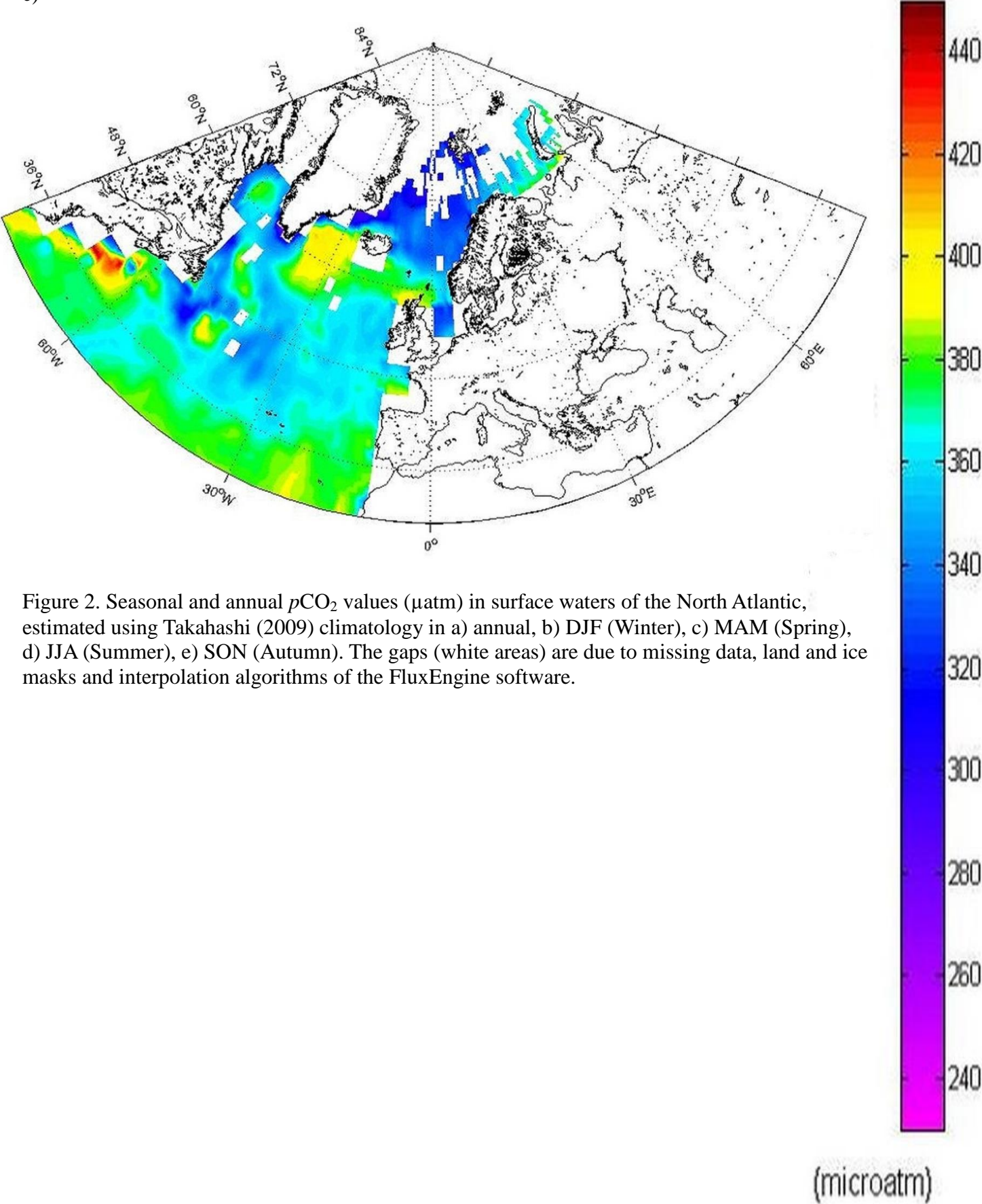
651  
652 d)



653  
654

(microatm)

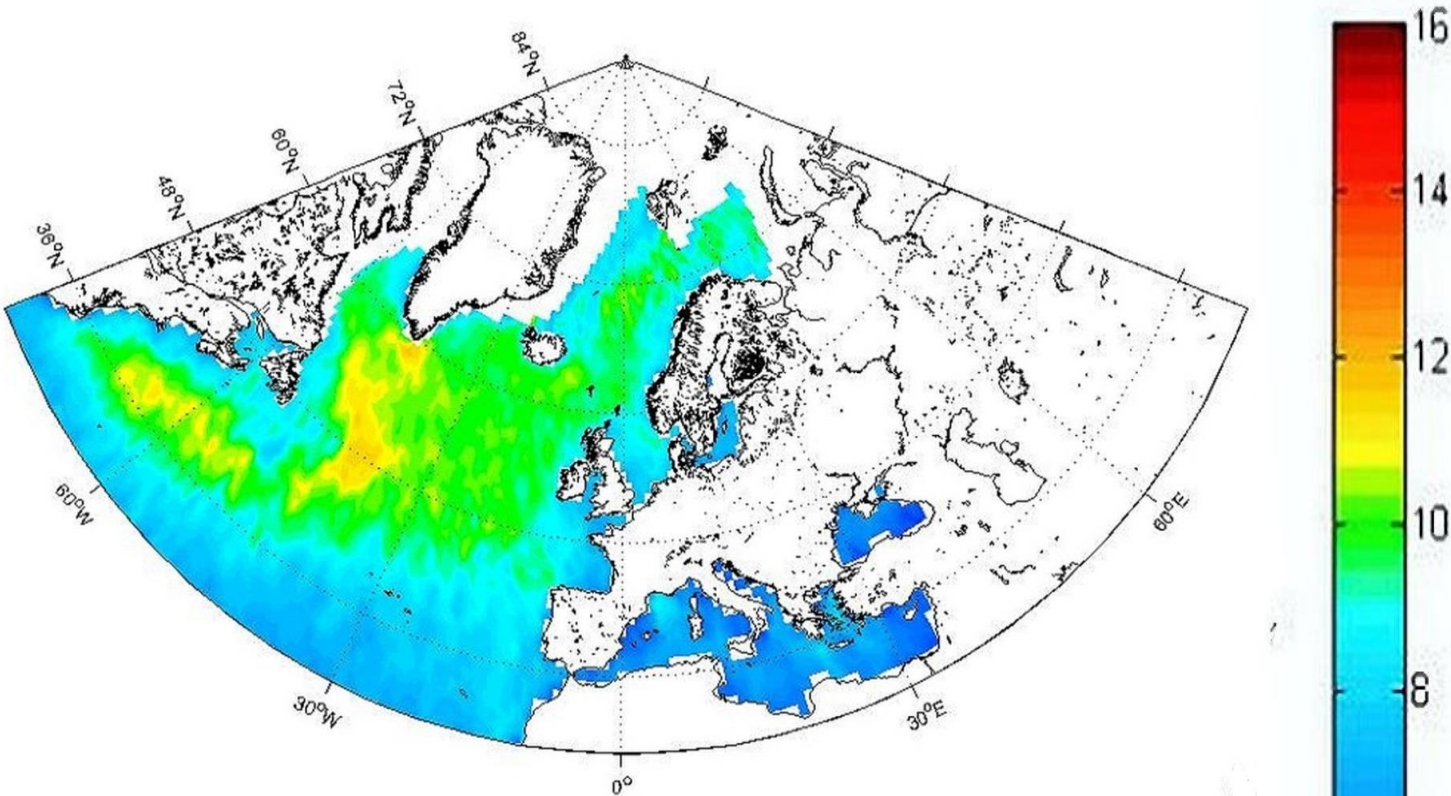
655  
656 e)



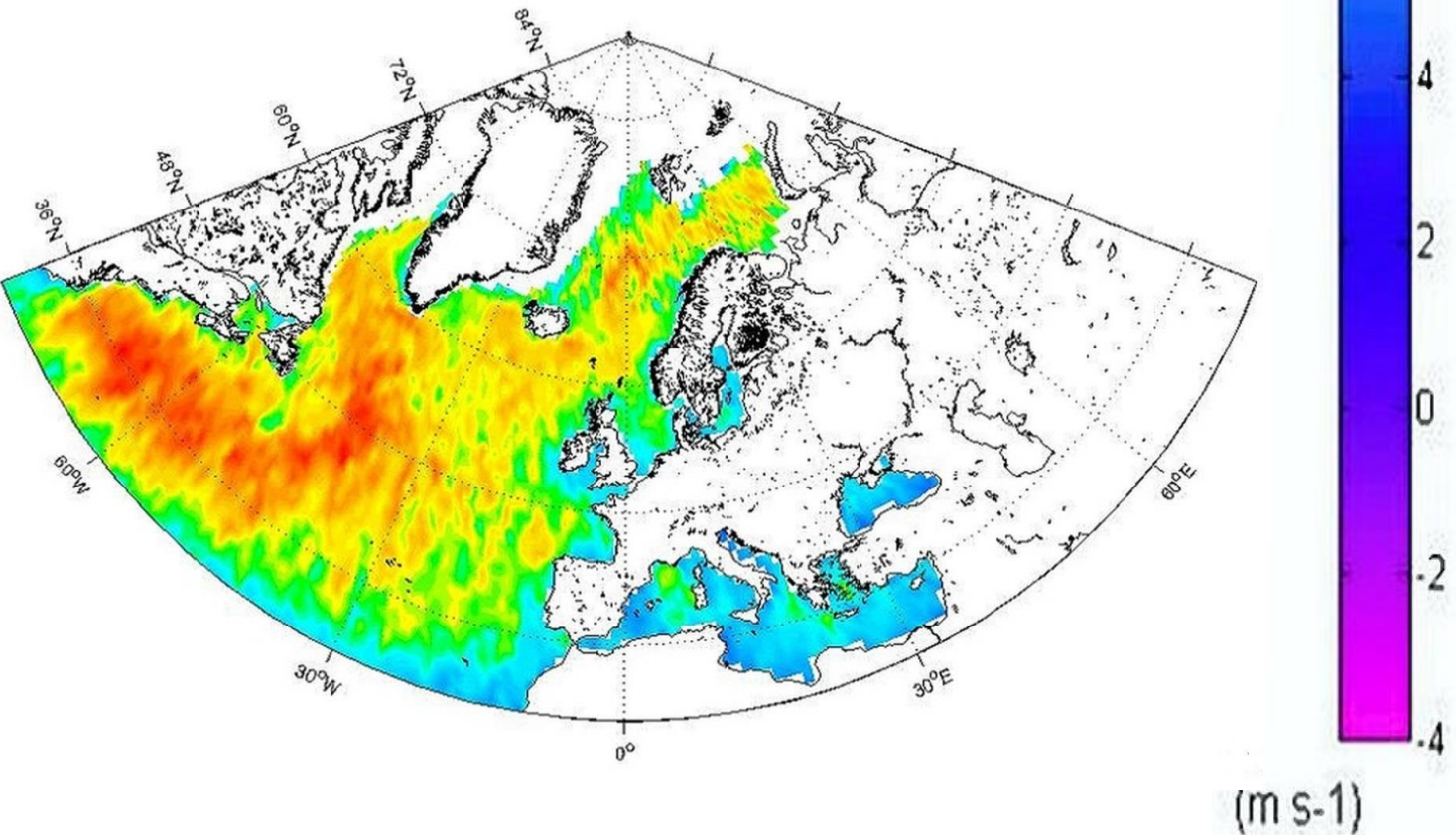
657  
658 Figure 2. Seasonal and annual  $p\text{CO}_2$  values ( $\mu\text{atm}$ ) in surface waters of the North Atlantic,  
659 estimated using Takahashi (2009) climatology in a) annual, b) DJF (Winter), c) MAM (Spring),  
660 d) JJA (Summer), e) SON (Autumn). The gaps (white areas) are due to missing data, land and ice  
661 masks and interpolation algorithms of the FluxEngine software.  
662  
663



664  
665 a)

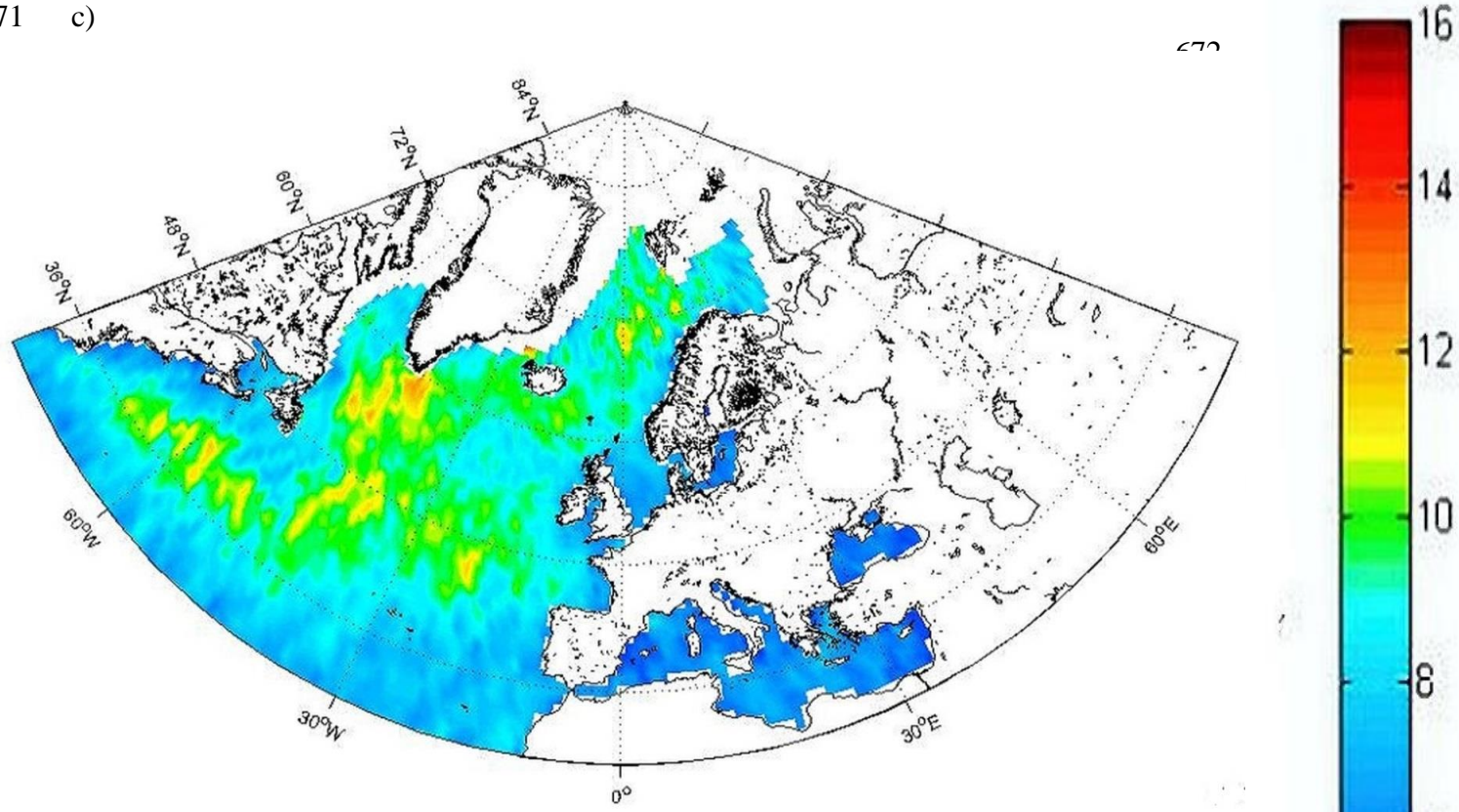


666  
667 b)

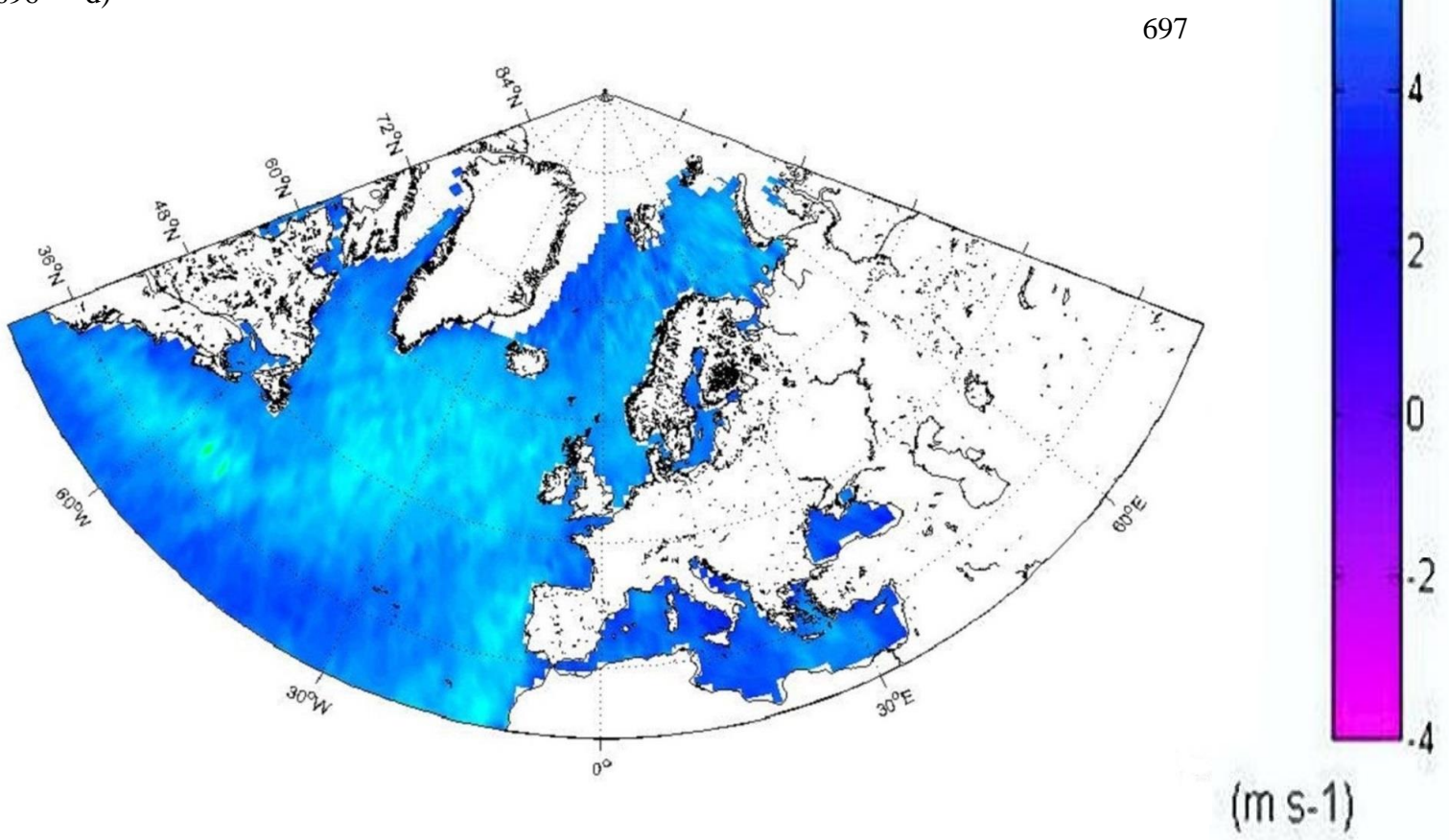




669  
670  
671 c)

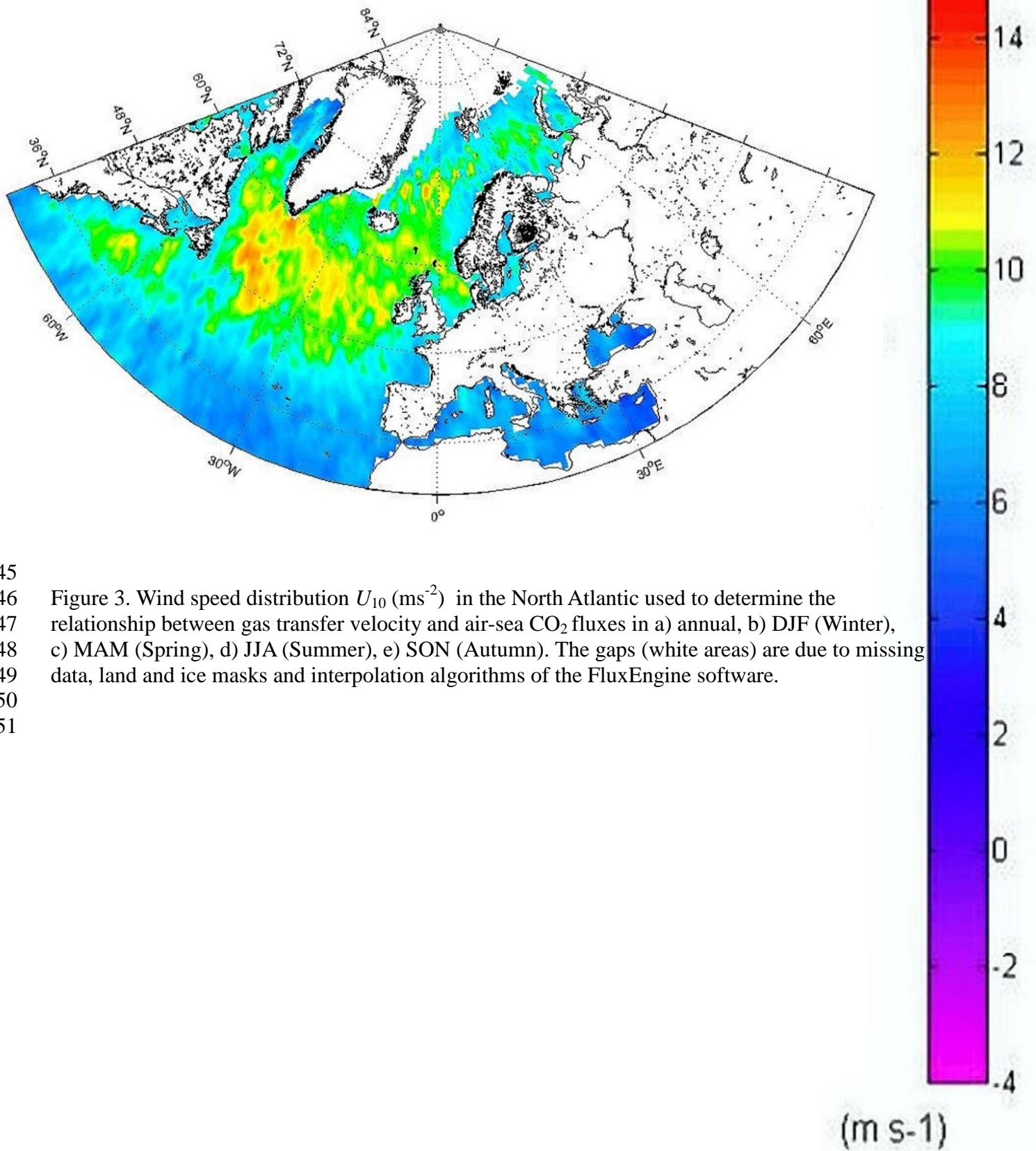


695  
696 d)



720  
721 e)

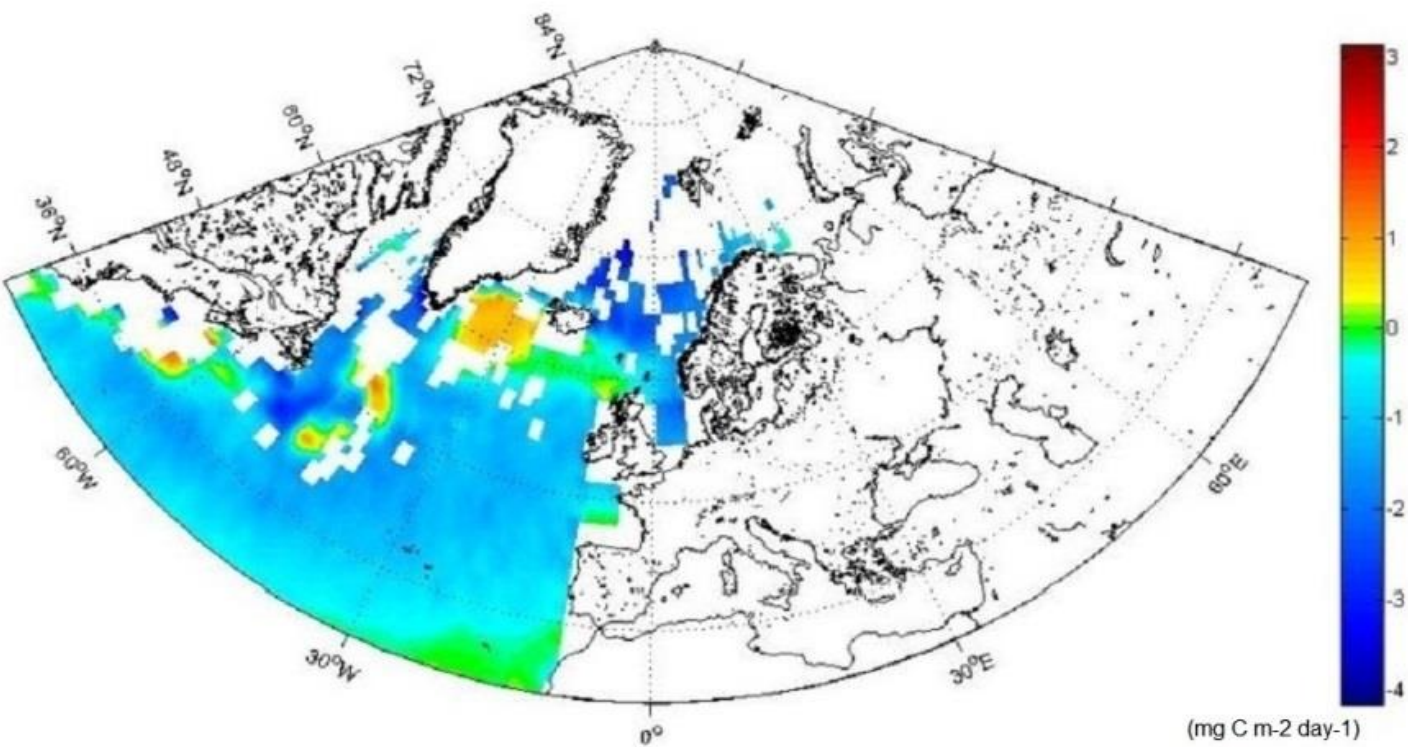
722



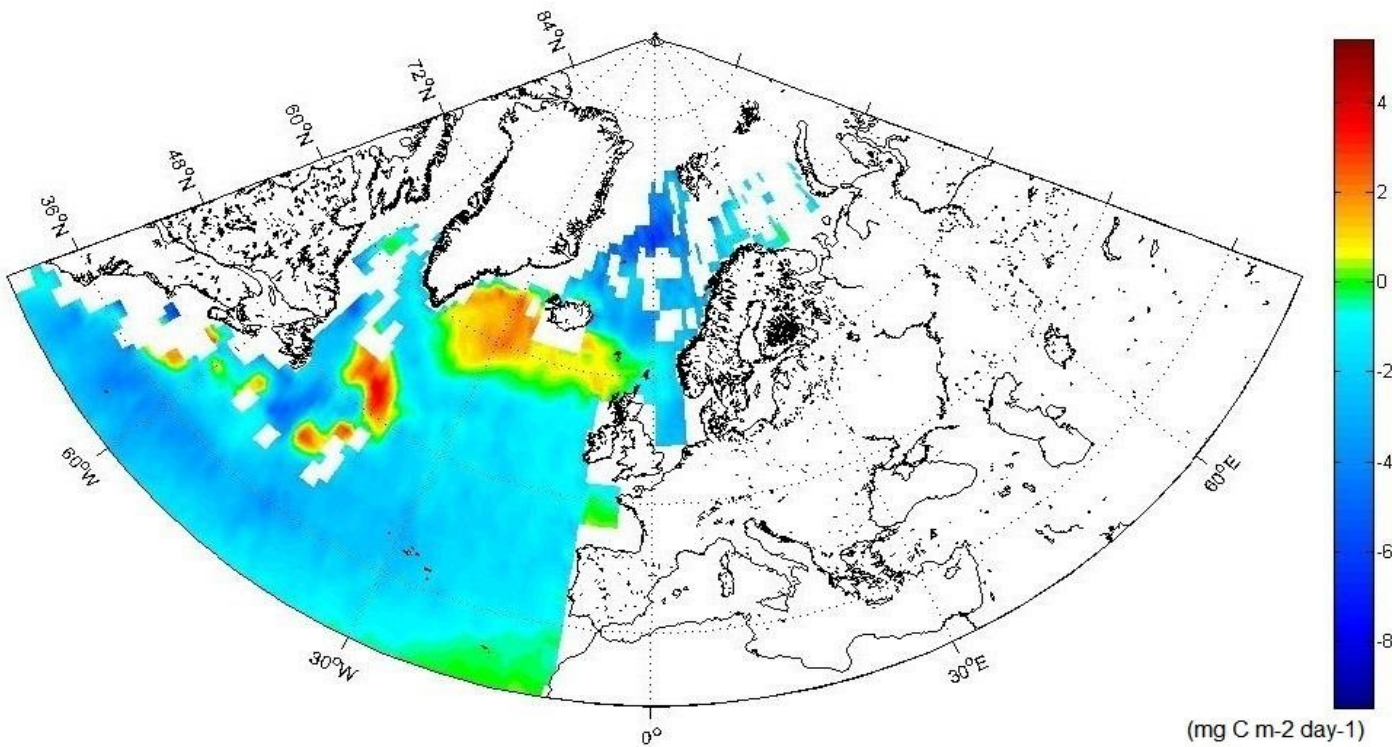
745  
746 Figure 3. Wind speed distribution  $U_{10}$  ( $\text{ms}^{-2}$ ) in the North Atlantic used to determine the  
747 relationship between gas transfer velocity and air-sea  $\text{CO}_2$  fluxes in a) annual, b) DJF (Winter),  
748 c) MAM (Spring), d) JJA (Summer), e) SON (Autumn). The gaps (white areas) are due to missing  
749 data, land and ice masks and interpolation algorithms of the FluxEngine software.  
750  
751



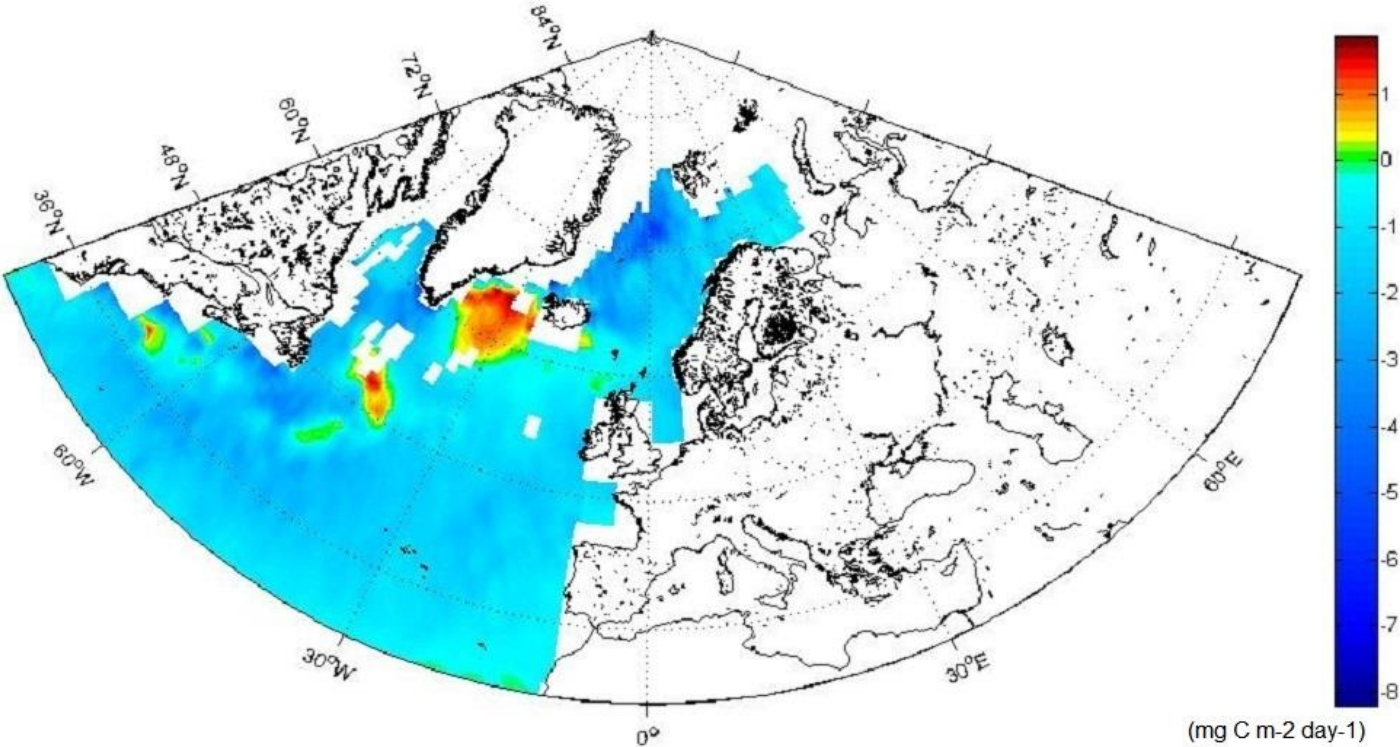
752  
753 a)



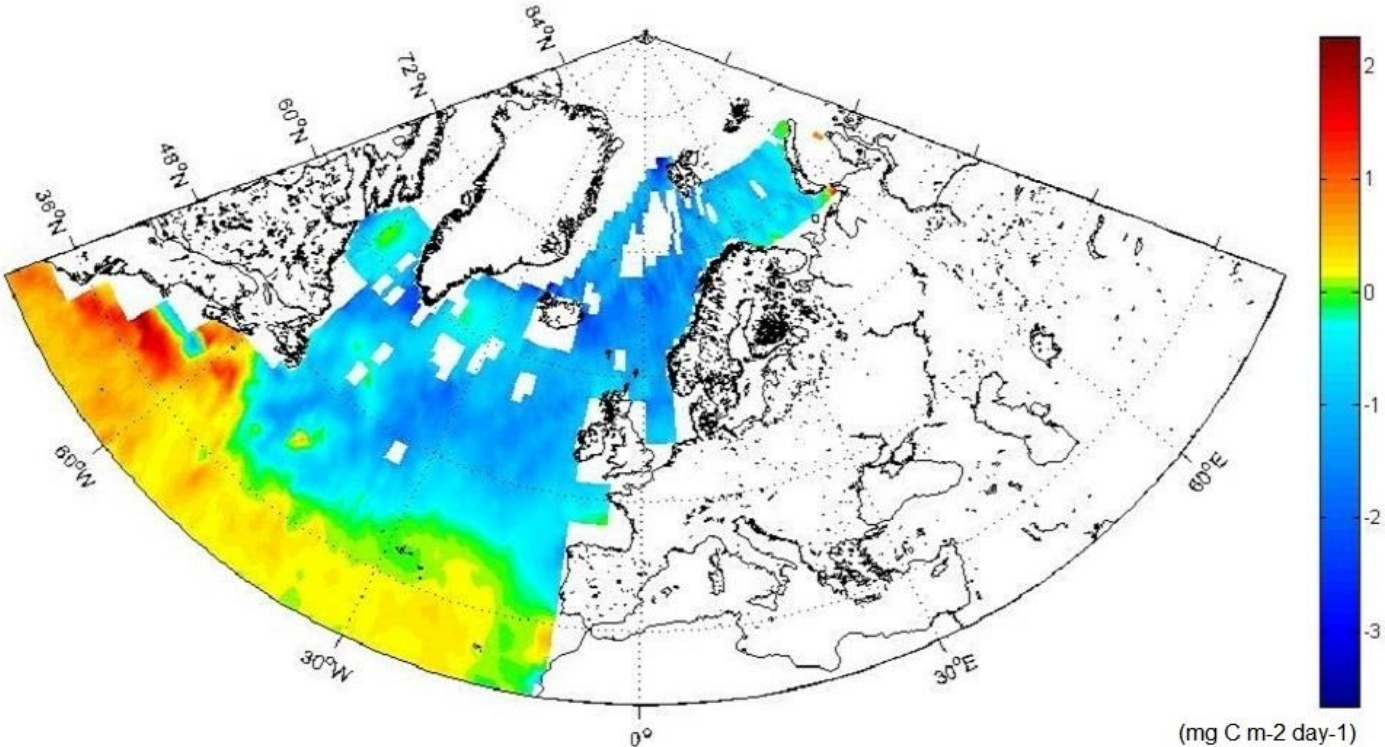
754  
755 b)



758  
759 c)

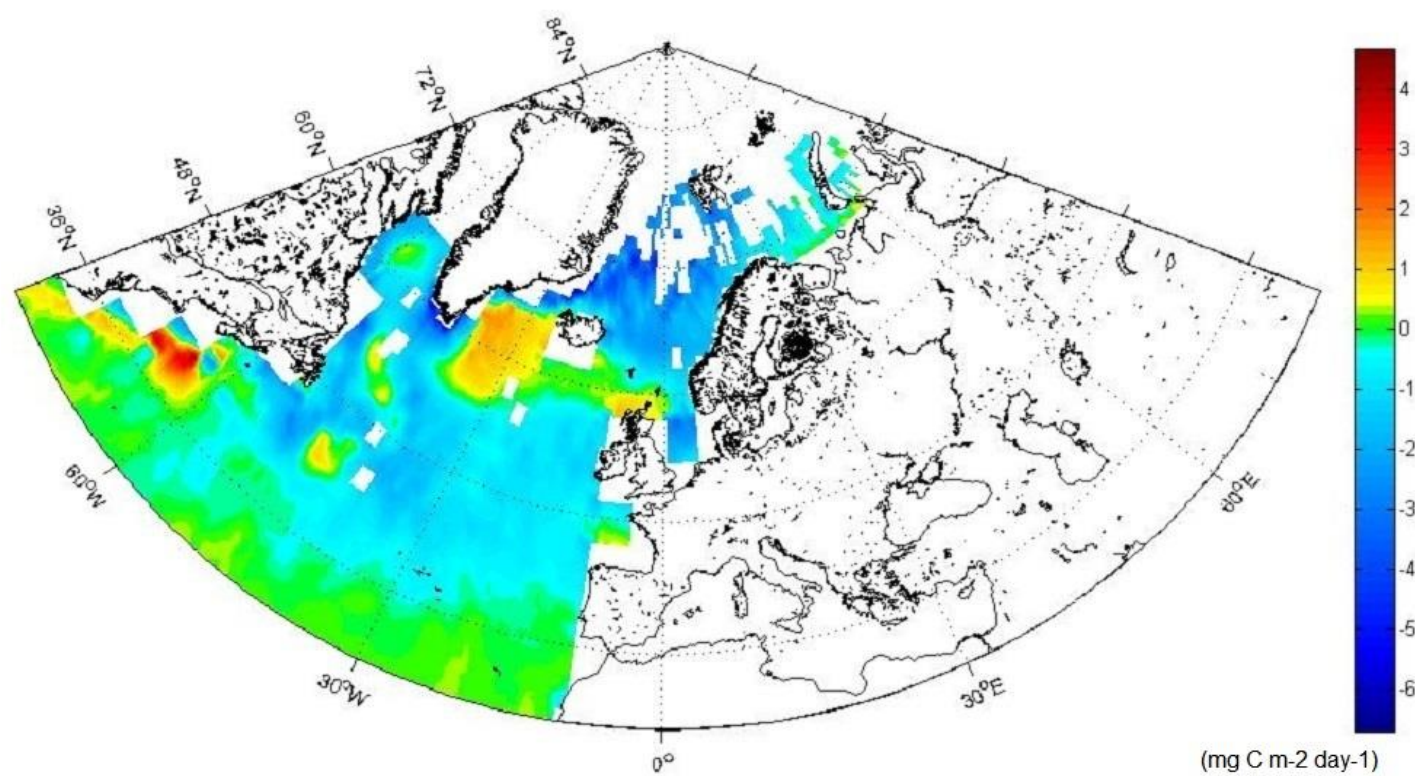


760  
761 d)





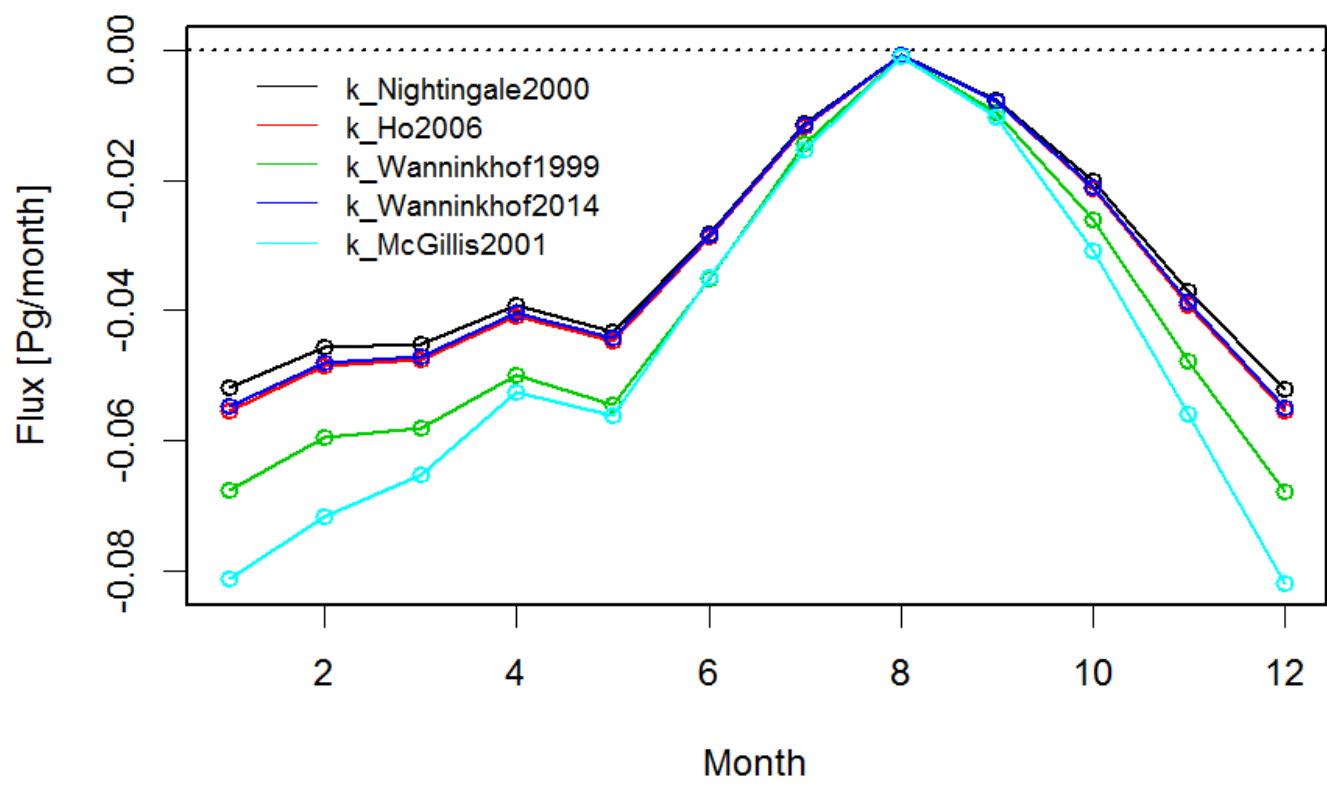
764  
765 e)



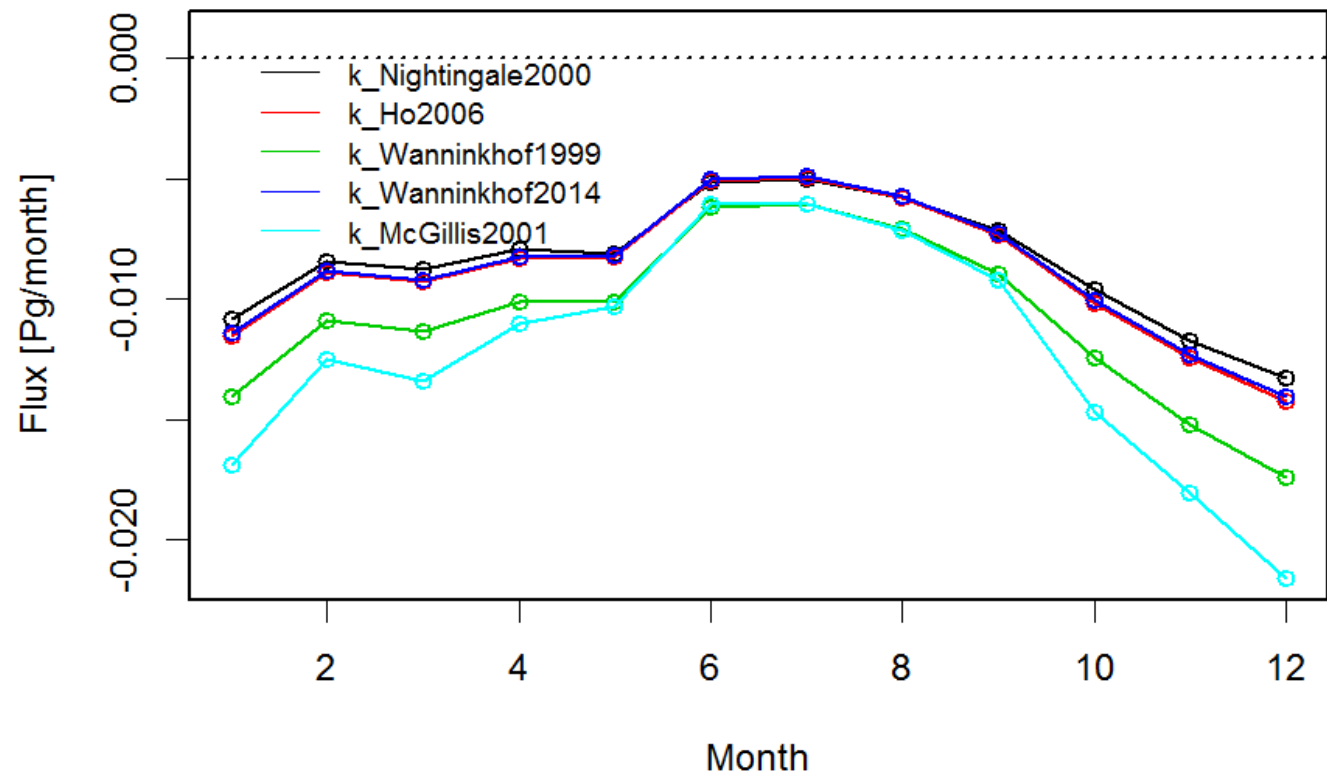
766  
767 Figure 4. Differences maps for the air-sea CO<sub>2</sub> fluxes (mg C m<sup>-2</sup> day<sup>-1</sup>) in the North Atlantic,  
768 between a wind cubed and squared parameterizations (Wanninkhof and McGillis 1999 and  
769 Wanninkhof 2014) in a) annual, b) DJF (Winter), c) MAM (Spring), d) JJA (Summer), e) SON  
770 (Autumn). The gaps (white areas) are due to missing data, land and ice masks and interpolation  
771 algorithms of the FluxEngine software.



772  
773 a)

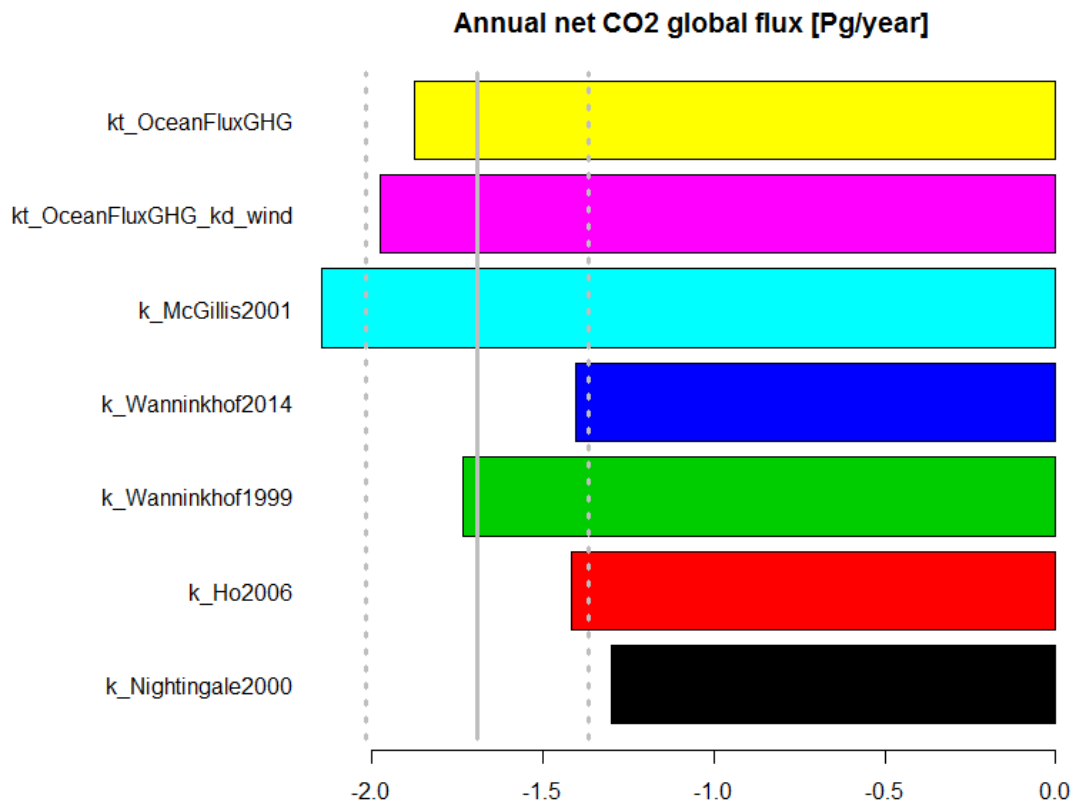


774  
775 b)

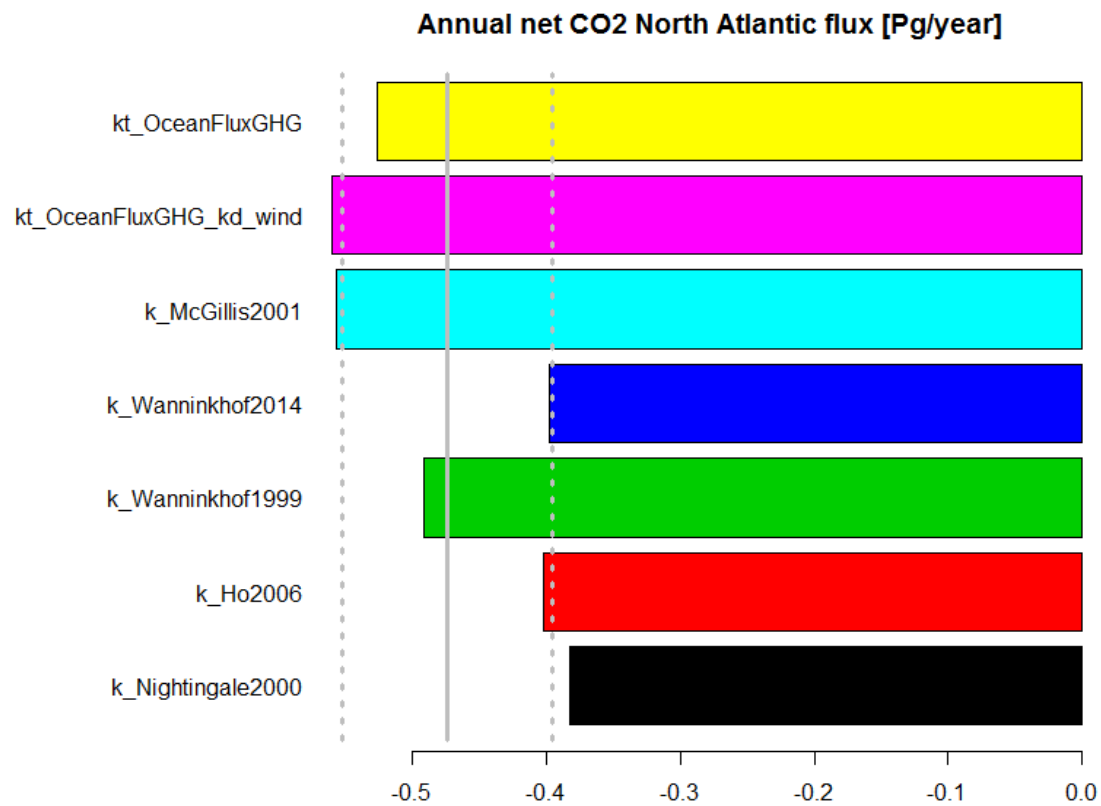


776  
777 Figure 5. Monthly values air-sea fluxes of CO<sub>2</sub> (Pg/month) for the five parameterizations (eq. 4-8)  
778 in a) North Atlantic, b) European Arctic.

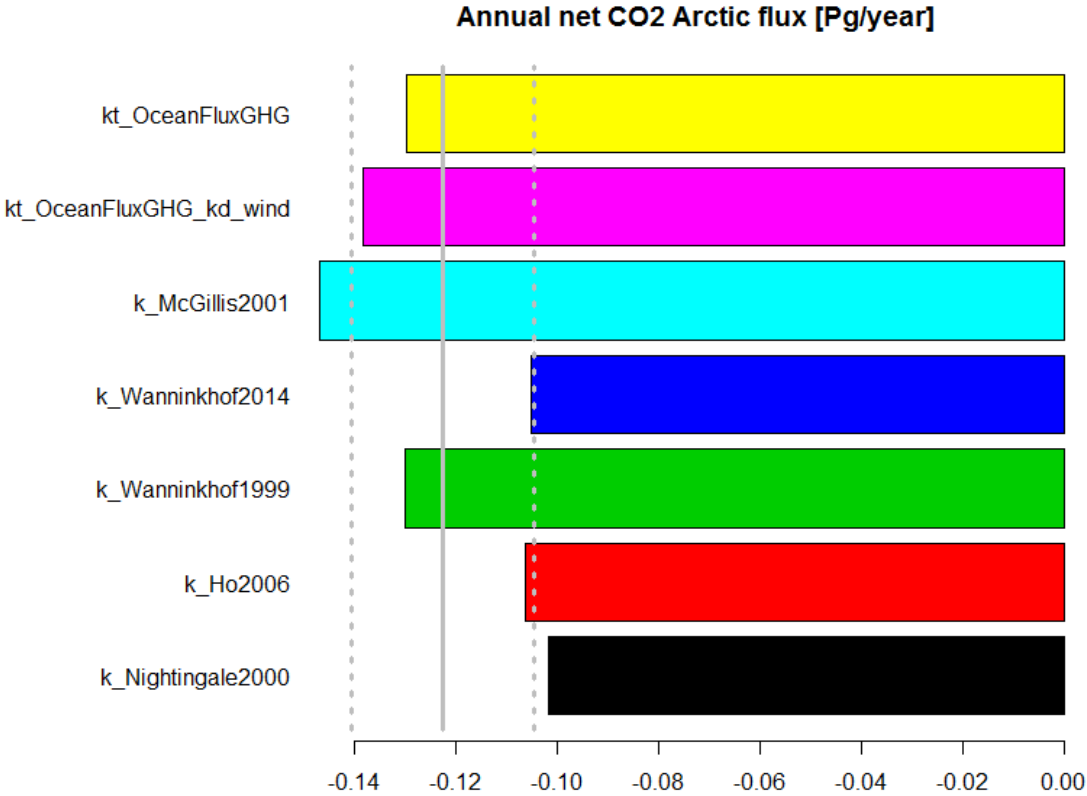
779  
780 a)



781  
782 b)

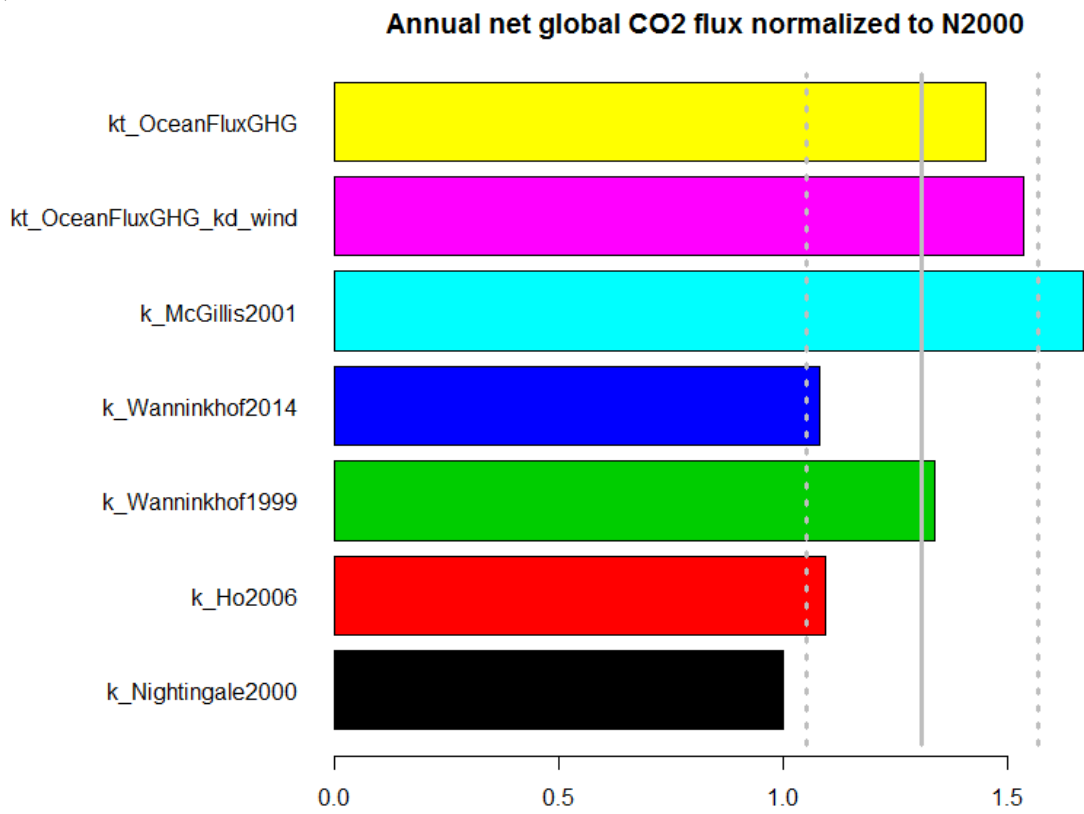


788  
789 c)

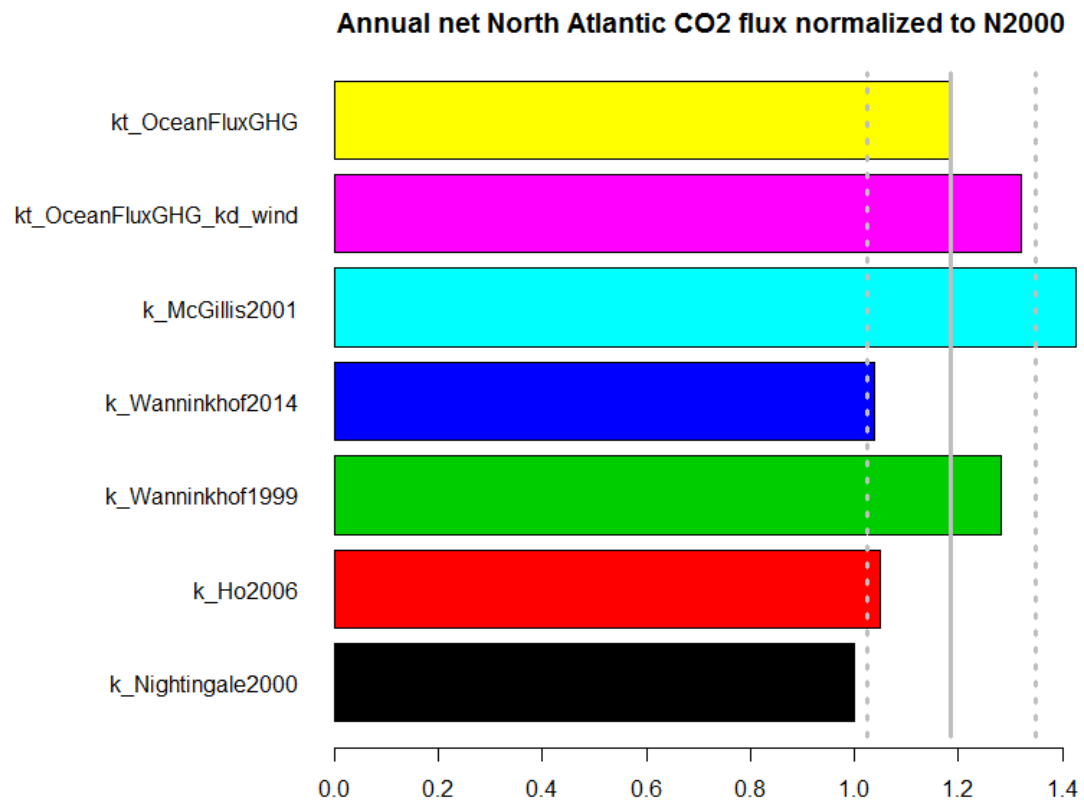


790  
791 Figure 6. Annual air-sea fluxes of CO<sub>2</sub> (Pg/year) for the five (eq. 4-8) parameterizations as well as  
792 for backscatter (default) and wind driven OceanFluxGHG parameterization (see text) in a) global, b)  
793 North Atlantic, c) European Arctic. Average values for all parameterization and standard deviations  
794 are marked as vertical gray lines.  
795

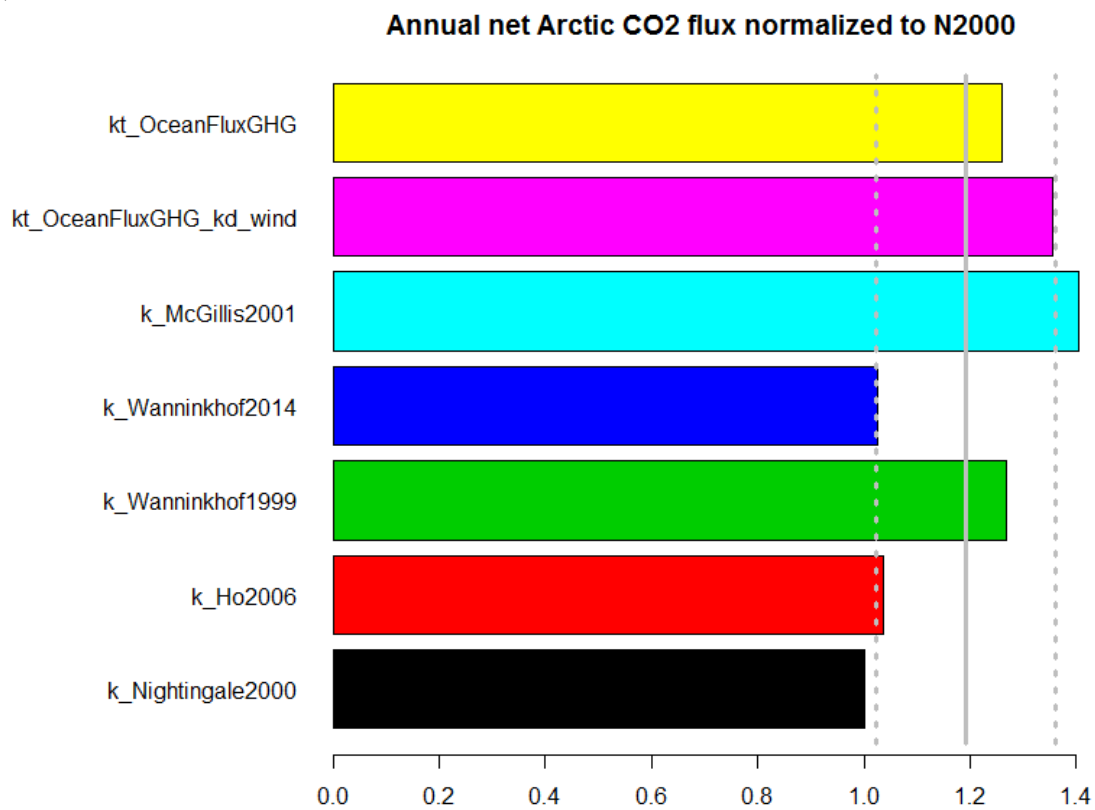
796  
797 a)



798  
799  
800 b)

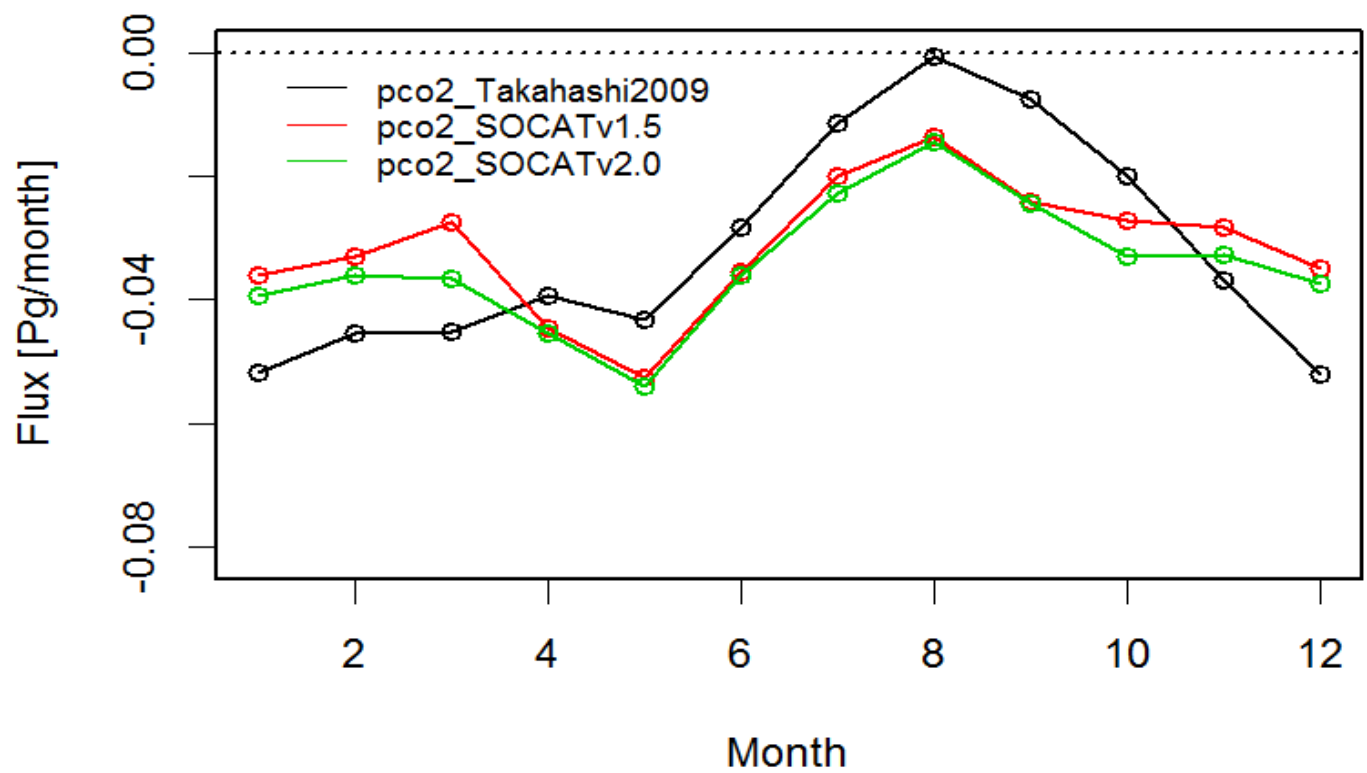


805  
806 c)

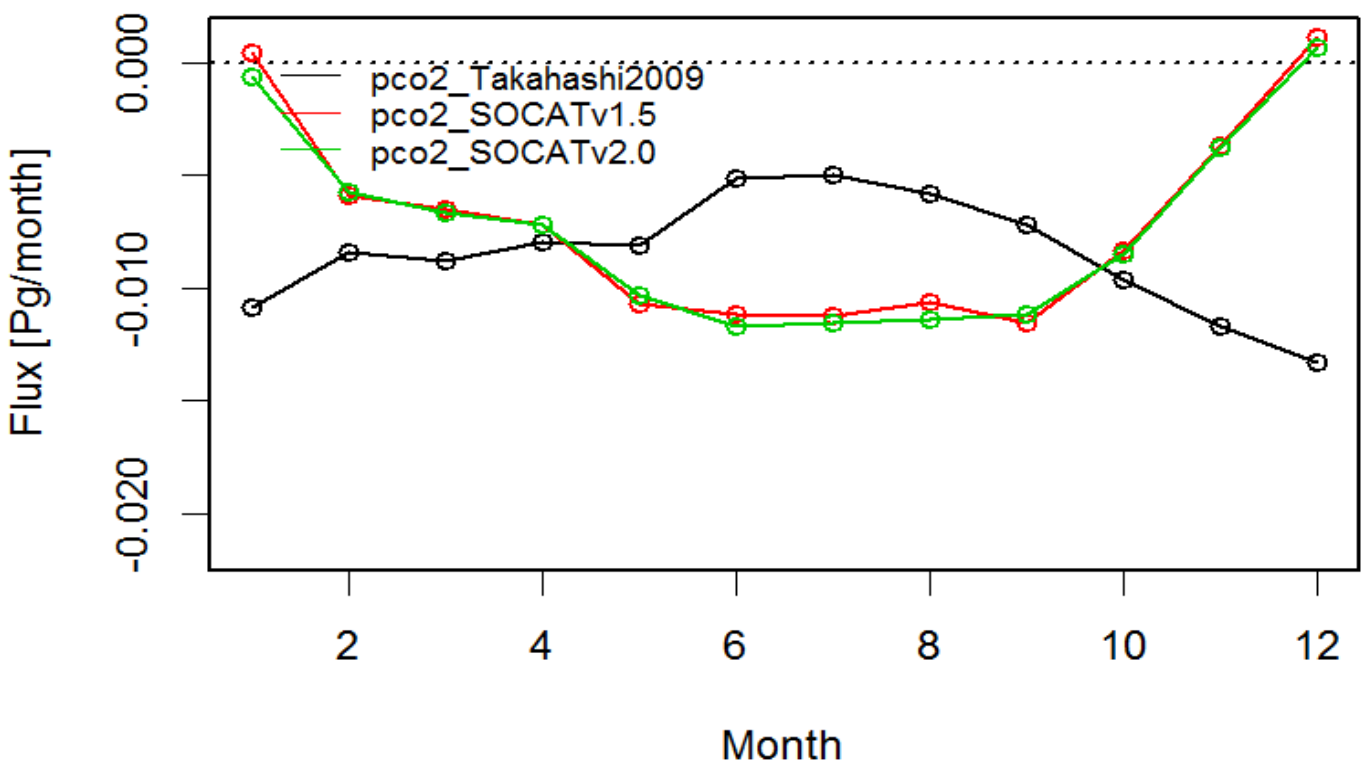


807  
808 Figure 7. Annual air-sea fluxes of CO<sub>2</sub> for the five (eq. 4-8) parameterizations as well as for  
809 backscatter (default) and wind driven OceanFluxGHG parameterization normalized to flux values  
810 of Nightingale et al. (2000) *k* parameterization.

811  
812 a)

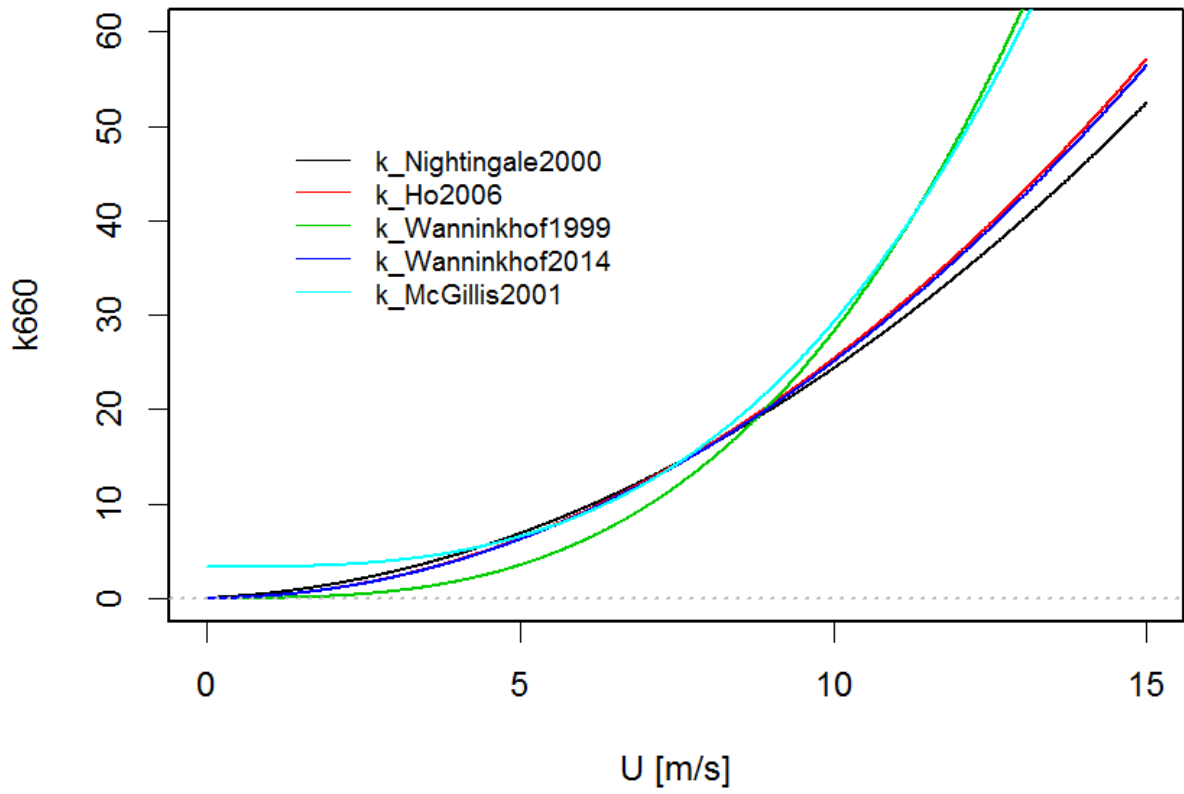


813  
814 b)



815  
816 Figure 8. Comparison of monthly values fluxes of air-sea CO<sub>2</sub> fluxes calculated with different  $p\text{CO}_2$   
817 datasets (Takahashi et al. 2009, SOCAT v. 1.5 and 2.0) using the same  $k$  parameterization  
818 (Nightingale et al. 2000) in a) North Atlantic, b) European Arctic.

819  
820



821  
822 Figure 9. Different k660 parameterizations as a function of wind speed.